Prepared for:

Rijkswaterstaat, Rijksinstituut voor Kust en Zee

DYNASTAR Project

A dynamic/empirical model for the long-term morphological development of estuaries

Development of the model, Phase II

November 1994

delft hydraulics

Prepared for:

Rijkswaterstaat, Rijksinstituut voor Kust en Zee

DYNASTAR Project

A dynamic/empirical model for the long-term morphological development of estuaries

Development of the model, Phase II

B. Karssen

November 1994

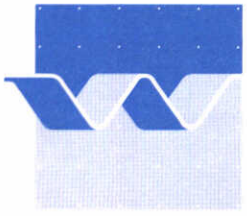

delft hydraulics

Executive summary

The Directoraat-Generaal Rijkswaterstaat/Rijksinstituut voor Kust en Zee of the Ministry of Public Works and Transport (RWS/RIKZ) is interested in morphological models predicting the consequences of (human) interference (e.g. dredging, land reclamation) in the geometry of estuaries and tidal basins.

In view of previous studies, the RWS decided to build a model for the long-term morphological development of estuaries (ESTMORF). Phase I of the development of ESTMORF was completed in January 1994. The present report contains a description of Phase II, during which the implementation of the software system is completed and models of the Westerschelde and the Friesche Zeegat are developed.

Comprehensive tests are performed with the software, in the form of debugging, prototype testing and real model testing, which have shown that the implementation of the software is correct, and according to the requirements of the model.

A set of pre- and post-processing programs is developed, which facilitates the use of the software system.

A morphological model is built of the Westerschelde, which is calibrated as good as possible using the available data and within the available time. Some qualitative features of the development of the Westerschelde are simulated properly and computed cross-sectional areas of channels compare reasonably well with observations.
The Westerschelde model is suitable for predictive purposes with respect to certain overall characteristics, such as the volume below mean (low or high) water level. However, the present model has to be considered as a first version or a working prototype. As more field data comes available and the behaviour of the development of estuaries is better understood, the model and the software will be improved in order to make the model suitable for more general predictive purposes as well.

A morphological model of the Friesche Zeegat has been set up and calibrated for the basin east of Engelsmansplaat. The results of the model are in very good agreement with observations. The morphological development of Zoutkamperlaag after the closure of the Lauwerszee in 1969 is simulated properly.
The predictive ability of the model is expected to be good. It can therefore very well be used to determine the future morphological development of the Zoutkamperlaag.

ESTMORF has proven to be a robust and flexible software system that is very suitable for research purposes in complex estuarine systems, such as the Westerschelde, but can also be used for consultancy with respect to more simple estuarine or tidal basin systems, such as the Friesche Zeegat.

Contents

List of symbols

A_c	=	cross-sectional area of the channel	[m^2]
A_h	=	cross-sectional area of the high tidal flat	[m^2]
A_l	=	cross-sectional area of the low tidal flat	[m^2]
A^{year}	=	cross-sectional are below MSL in year	[m^2]
c	=	sediment concentration by volume at a node	[-]
c_c	=	sediment concentration by volume in the channel	[-]
c_{ce}	=	equilibrium concentration by volume in the channel	[-]
c_h	=	sediment concentration by volume in the high tidal flat part	[-]
c_{he}	=	equilibrium sediment concentration by volume in the high tidal flat part	[-]
c_l	=	sediment concentration by volume in the low tidal flat part	[-]
c_{le}	=	equilibrium sediment concentration by volume in the low tidal flat part	[-]
D_c	=	dispersion coefficient channels	[m^2/s]
D_h	=	dispersion coefficient high flats	[m^2/s]
D_l	=	dispersion coefficient low flats	[m^2/s]
F_{lc}	=	exchange rate of sediment between the channel the low tidal flat	[m^2/s]
h_h	=	effective water depth for the high tidal flat	[m]
h_l	=	effective water depth for the low tidal flat	[m]
j	=	index of the branch	[-]
k	=	index of the node	[-]
L	=	length of a branch	[m]
L_{hl}	=	distance between the centre of the high flat and that of the low flat	[m]
L_{lc}	=	distance between the centre of the channel and that of the low flat	[m]
$N_{br,k}$	=	number of branches connected to node k	[-]
Q	=	discharge	[m^3/s]
S	=	sediment transport	[m^3/s]
t	=	time	[s]
u	=	residual flow velocity	[m/s]
x	=	horizontal coordinate	[m]
W_c	=	width of the channel	[m]
W_h	=	width of the high part of the tidal flat	[m]
W_l	=	width of the low part of the tidal flat	[m]
w_s	=	coefficient having the dimension of velocity	[m/s]
ΔA_r	=	relative area change	[-]

The following conventions are used in this report:

- A parameter subscript *j* denotes that the value of this parameter is at a branch (*j*).
- A parameter subscript *k* denotes that the value of this parameter is at a node (*k*).
- A parameter superscript *n* denotes that the value of this parameter is at the old (previous) time step (*n*).
- A parameter superscript *n+1* denotes that the value of this parameter is at the new (present) time step (*n+1*).

List of figures

List of tables

1 Introduction

The Directoraat-Generaal Rijkswaterstaat/Rijksinstituut voor Kust en Zee of the Ministry of Public Works and Transport (RWS/RIKZ) is interested in morphological models predicting the consequences of (human) interference (e.g. dredging, land reclamation) in the geometry of estuaries and tidal basins.

Two types of models are considered:

- a one-dimensional middle long-term model to predict the morphological development in estuaries and tidal basins for a period of 20 to 30 years.
- a one-dimensional long-term model to predict the morphological development in estuaries and tidal basins for a period of 50 to 100 years.

The middle long-term model (called EENDMORF) is studied in the project DYNASTAR. In the framework of EENDMORF, a study of the proper nodal relations - defining the distribution of sediment over the branches at a bifurcation - to be applied in the model to be developed is just completed by DELFT HYDRAULICS. This study is funded by the Directoraat-Generaal Rijkswaterstaat/Directie Zeeland of the Ministry of Public Works and Transport.

The long-term model (called ESTMORF), which is the subject of this report, is also studied in the project DYNASTAR. For the latter RWS/RIKZ commissioned DELFT HYDRAULICS in August 1991 to perform a preliminary study and a literature survey on the subject of the long-term model, as part of the project DYNASTAR. These studies were completed with a note and a report, respectively (Karssen and Wang, 1991a/b).

In Karssen and Wang (1991a, 1991b) two concepts are evaluated for a dynamic-empirical morphological model like ESTMORF: the concept of Di Silvio and the concept of Allersma. Both concepts have their advantages and disadvantages. In Karssen and Wang (1991b) it was concluded that a combination of both concepts in one model would probably result in a model with the required properties.

In Karssen and Wang (1992) the 'combined' model concept described above is worked out and it is compared with a concept based on the model of van Dongeren (1992). It was recommended to choose this combined concept for the development of the model.

In the framework of the ISOS*2-project Eysink (1992) formulated another concept which uses a more sophisticated schematisation of the geometry but uses a less sophisticated formulation for the sediment transport process than in the concept suggested by Karssen and Wang (1992).

In November 1992, RWS/RIKZ commissioned DELFT HYDRAULICS to carry out a part of the development of the model. That part contained the verification of the choice of the model concept and the elaboration of the physical relations in the model in detail taking into account the work carried out in the ISOS*2-project (Eysink, 1992). The study was completed with a report (Karssen and Wang, 1993).

In view of the previous studies, the RWS decided to build the model. With letter AOE/936522 dated 29 July 1993, RWS/RIKZ commissioned DELFT HYDRAULICS to perform the following activities:

- Phase I:
  Development of the ESTMORF-software, preparation of a dedicated model of both the Westerschelde and the Friesche Zeegat and performance of first tests with the software.

- Phase II:
  Performance of extensive tests with the software, calibration of the models, sensitivity analyses and implementation of the software at the clients' office.

Two changes to the above list of activities were made in close concert with the client:

- During execution of Phase I it became clear that branches without tidal flats were present in the Westerschelde IMPLIC-model. Furthermore, these branches consisted of a channel with vertical walls. The physical relations described in (Karssen and Wang, 1993) did not foresee in such a geometry. It was therefore decided to extend the solution method of the concentration field and the changes in the cross-sectional area in order to make morphological computations using this channel geometry possible.

- The preparation of the dedicated models of the Westerschelde and the Friesche Zeegat already required comprehensive tests with the software. It was therefore decided to perform these tests during Phase I instead of during Phase II.

In Karssen (1994), the results of Phase I of the study are laid down.

The following activities were part of Phase II of the study:
- A brief sensitivity analysis for schematic prototypes in order to get a feeling for the values of the parameters.
- Prototype tests for sea level rise and land subsidence.
- Programming of output procedures.
- Calibration of the Westerschelde model.
- Calibration of the Friesche Zeegat model.
- Preparation of a report.
- Delivery of the software to the client.

This report contains a description of the above activities such as performed during Phase II. In Chapter 2 a general description of the software is given. Chapter 3 contains an overview of the sensitivity analyses that were performed and the results of prototype tests related to sea level rise and land subsidence. The results of the calibration of the Westerschelde model and the Friesche Zeegat model can be found in Chapter 4 and Chapter 5, respectively. Finally, in Chapter 6 the conclusions and recommendations are summarised.

It is noted that the *use* of the ESTMORF software (including post-processing software) and the format of the input and output files will be worked out in a separate User Manual.

This study was performed by R. Bruinsma and B. Karssen under the guidance of A. Langerak from RWS. The report is drawn up by B. Karssen.

2 Description of the software

2.1 Introduction

In the Phase I report (Karssen, 1994), it was mentioned that only minor changes may be necessary during Phase II, and that the overall description of the software such as given in that report could be considered as final. This statement has been proven to be true during Phase II; the overall structure is unchanged. However, minor changes are made in the software. These changes can be divided in the following categories:

- improvement of existing modules and small errors,
- speeding up and improved flexibility of the computational process,
- input procedures of the impact of human interference,
- output procedures, and
- user-friendliness.

Due to the above changes, new modules are added and old modules are adapted.

In this chapter the resulting general structure of the software is described (see Section 2.2). Section 2.3 presents the two computational methods that are implemented in the software. A detailed description of the software and its use, including a full description of the input and output files, can be found in the User Manual.

2.2 General structure of the software

One of the purposes of ESTMORF is to compute the morphological development in estuaries after (human) interference, starting from an equilibrium situation. The difficulty in this case is how to determine the equilibrium constants which are defined by this equilibrium situation. This is important as they - on their turn - define the equilibrium situation(s) during the simulation. In some cases, such as for the Westerschelde and the Friesche Zeegat, uniform equilibrium constants have been determined in previous studies as average values for the whole estuary and over the individual branches. This will not lead to a well-defined equilibrium in all branches as there is a substantial spreading in the data.

As the equilibrium constants depend on the hydrodynamics and the geometry in the equilibrium situation, these constants can very well be determined by the software itself. This feature has been built in in the ESTMORF-software.

The above leads to two types of ESTMORF-simulations that can be distinguished:

- a 'simulation' to compute the equilibrium constants, and
- a simulation to compute the morphological development.

Details of the simulation to compute the equilibrium constants are worked out in the User Manual. A description of 'normal' morphological simulations can be found below.

A morphological simulation with ESTMORF basically consists of the following steps:

1. A hydrodynamic simulation (using IMPLIC), which is performed to determine:
   - the inflowing and outflowing volumes of water during a tidal cycle, and
   - the mean high water level (MHW), mean sea level (MSL) and the mean low water level (MLW)

   at the beginning and at the end of each branch.
   Above values are used in empirical relations to determine the equilibrium values of several parameters.
2. The computation of the morphological changes. Based on the new equilibrium values, the sediment transport is computed, followed by the computation of the change in cross-sectional area. This is repeated until the morphological change is large enough to have effect on the hydrodynamics.

The period during which the hydrodynamics are assumed to be constant is to be given by the user. When this period has elapsed, the whole cycle consisting of Step 1 followed by Step 2 is repeated. On its turn, this cycle is repeated until the simulation end time is reached.

At the beginning of the computation two problems may occur:

- The first period of a hydrodynamic computation is hampered by the initial conditions. The software therefore makes it possible to run an IMPLIC simulation first until the effect of the initial conditions have disappeared from the hydrodynamic parameters solved. After this 'spin-up period' the results of the hydrodynamic model can be used by the morphological module to determine ESTMORF cross-sectional profiles.

- The first time a morphological computation is performed with the spun-up hydrodynamic model, the schematic ESTMORF cross-sectional profile (consisting of 7 points in the vertical) has not yet been determined, because the coordinates of some of these points depend on the hydrodynamic results. During the testing phase, the problem arose that after one conversion of the IMPLIC-profile (consisting of 20 points in the vertical) to the ESTMORF-profile (7 points), the hydrodynamic results did change, which on their turn changed the ESTMORF-profile. Although the changes are small, this means that even without morphological changes, the profiles change due to the conversion and the impact of this conversion on the hydrodynamics.
  This 'problem' was solved by implementing an iterative procedure at the start of the simulation, during which the IMPLIC-profile and the ESTMORF-profile are converted until an approximately stable situation has been reached. The differences between the original hydrodynamics and the hydrodynamics after the iteration procedure are small. A thorough description of this feature and the implemented iteration procedure can be found in the User Manual.

During the actual morphological computation (Step 2, see previous page), the following sequence of activities is performed:

1. Compute the present cross-sectional areas from the present ESTMORF-profiles.
2. Read in the tidal volumes and the water levels from the output of IMPLIC.
3. Compute the new ESTMORF-profiles due to a possible change in water levels and land subsidence (no transport; see Karssen and Wang, 1993).
4. Compute the new cross-sectional areas and widths.
5. Compute the new equilibrium values for the heights of the tidal flats, the cross-sectional area below MSL and the concentration field.
6. Read in the new boundary conditions for the concentration.
7. Compute the sediment transport and the new concentration field.
8. Compute the sedimentation/erosion.
9. Compute the new cross-sectional areas and the new ESTMORF-profiles.
10. Repeat steps 4. through 9. until human interference, land subsidence or when a new hydrodynamic computation is necessary.
11. Read in the changes due to human interference and compute the new ESTMORF-profiles.

2.3 Two computational methods

Two computational methods are possible: an implicit and an explicit method.
An implicit scheme looks very promising from the stability point of view, but will lead to the use of complicated one-dimensional network solvers. The gain on the magnitude of the time step may be compensated by the loss on computational time needed to solve the system of differential equations. Another disadvantage is the complexity of the software and the maintenance.
An explicit scheme facilitates the testing of the software and will lead to less computational effort per simulation. However, using an explicit method leads to stability criteria that have to be met. One of the main problems with respect to this is due to the source terms in the transport equations.

The main requirement of the two implemented computational methods is simple: the computational method should compute the new cross-sectional profiles in the area of interest (which is the model area, such as the Westerschelde and the Friesche Zeegat) based on the physical relations as described in (Karssen and Wang, 1992; Karssen and Wang, 1993).

An additional requirement is that the computational effort needed for a simulation should be as small as possible. This means that the numerical scheme should be stable for reasonably large time steps and thereby providing sufficient accuracy.

In view of the above, it was decided to implement two different computational methods for the computation of the concentration field from which the user can choose:

1. A semi-explicit scheme consisting of a central differences scheme, combined with implicit source terms to solve the concentration in the internal points of the branches. This scheme is solved by iteration, leading to a steady solution per morphological time step. (See Section 2.3.1).

2. A central difference scheme solving the boundary value problem (obtained by setting the time derivative to zero in the transport equation).
   The boundary values (the nodes of each of the branches) are determined from the concentration field of the previous time step. Iteration leads to the final solution. (See Section 2.3.2).

For both methods, an explicit numerical scheme (Euler's method) is used to solve the sedimentation/erosion field. Method 1 and the computation of the cross-sectional area change have already been worked out in Karssen (1994). For the sake of completeness, these methods are again presented in this section.

It is noted that the cross-sectional areas are assumed to remain unchanged during the computation of the concentration field.

2.3.1 Method 1: Iteration to steady state

In this method, the computation of the concentration field is an iterative process, which leads to a (quasi-)steady concentration field, i.e. a concentration field which is steady during one morphological time step, but (of course) not steady during the whole morphological computation.

The time step of the iterative solution method for the (quasi-)steady concentration field is small (minutes) compared with the morphological time step (days/months/years).

Graphically, the iterative process can be presented as follows:

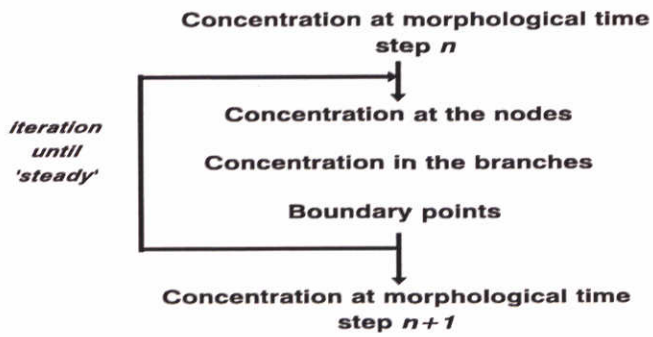

The computation of the concentration field within the iterative process is described below.

Nodes

First, the concentration in the nodes is computed. In the nodes the continuity equation for the sediment must hold, i.e. the incoming sediment transport must equal the outgoing sediment transport:

$$\sum_{j=1}^{N_{br,k}} S_j = \sum_{j=1}^{N_{br,k}} \left(Q_j\, c_k - A_{c,j}\, D_{c,j} \frac{\partial c_{c,j}}{\partial x} \right) = 0 \qquad (2.1)$$

where:

A_c	=	cross-sectional area of the channel	[m^2]
c_c	=	sediment concentration by volume in the channel	[-]
c	=	sediment concentration by volume in a node	[-]
D_c	=	dispersion coefficient for the channel	[m^2/s]
j	=	index of a branch	[-]
k	=	index of a node	[-]
$N_{br,k}$	=	number of branches connected to node k	[-]
Q	=	discharge	[m^3/s]
S	=	sediment transport	[m^3/s]
x	=	horizontal coordinate	[m]

In view of the fact that the continuity equation for the water is already satisfied (the discharges originate from an IMPLIC-run), this leads to the following numerical relation for the concentration in the nodes that are not boundary points:

$$c_k^{n+1} = \frac{\sum_{j=1}^{N_{br,k}} \left(\frac{A_j\, D_j}{L_j}\, c_{c,j}^{n} \right)}{\sum_{j=1}^{N_{br,k}} \left(\frac{A_j\, D_j}{L_j} \right)} \qquad (2.2)$$

where:

L_j	=	length of branch j	[m]

It is noted that the superscript *n+1* denotes the new time step, whereas the superscript *n* denotes the previous time step.

Branches

Then the concentration in the branches is computed. Two cases must be distinguished:

- the branches for which sediment transport from and to the tidal flats should be included (case A)
- the branches for which no sediment transport from and to the tidal flats takes place (case B)

The user should specify the above status of the branches in the model schematization before running the ESTMORF-model.

Case A: Tidal flats included

The mass balance equation for sediment in the channel can be written by:

$$\frac{\partial A_c c_c}{\partial t} + \frac{\partial A_c u c_c}{\partial x} - \frac{\partial}{\partial x}\left(A_c D_c \frac{\partial c_c}{\partial x}\right) = W_c w_s (c_{ce} - c_c) + F_{lc} \qquad \textbf{(2.3)}$$

where:

c_{ce}	=	equilibrium concentration by volume in the channel	[-]
F_{lc}	=	exchange rate of sediment between the channel the low tidal flat, which is defined positive if transport occurs from the tidal flat to the channel	[m²/s]
t	=	time	[s]
u	=	residual flow velocity	[m/s]
W_c	=	width of the channel	[m]
w_s	=	coefficient having the dimension of velocity	[m/s]

The sediment flux from the tidal flat to the channel F_{lc} is elaborated as follows:

$$F_{lc} = D_l \, h_l \, \frac{c_l - c_c}{L_{lc}} \qquad \textbf{(2.4)}$$

where:

c_l	=	sediment concentration by volume in the low tidal flat part	[-]
D_l	=	diffusion coefficient low flats	[m²/s]
L_{lc}	=	distance between the centre of the channel and that of the low flat	[m]
h_l	=	effective water depth for the low tidal flat	[m]

By the use of a central differences scheme, combining Equations (2.3) and (2.4) and by taking the source terms (the right hand side of Equation (2.3)) implicit, the following expression is found:

$$\left(A_c^n + W_c \, w_s \, \Delta t + \frac{D_l \, h_l}{L_{lc}} \, \Delta t \right) c_c^{n+1} - \frac{D_l \, h_l}{L_{lc}} \, \Delta t \, c_l^{n+1}$$

$$= \qquad \textbf{(2.5)}$$

$$A_c^n \, c_c^n + W_c \, w_s \, \Delta t \, c_{ce} - \frac{S_2 - S_1}{L} \, \Delta t$$

where:

$$S_2 = A_{c,2}^n \, u_2 \, c_{k,2} - \frac{A_{c,2}^n \, D_c}{0.5 \, L} \left(c_{k,2}^{n+1} - c_c^n \right)$$

$$S_1 = A_{c,1}^n \, u_1 \, c_{k,1} - \frac{A_{c,1}^n \, D_c}{0.5 \, L} \left(c_c^n - c_{k,1}^{n+1} \right) \qquad \textbf{(2.6)}$$

It is noted that the subscript 2 refers to the end of the branch, whereas subscript 1 refers to the beginning of the branch.

The mass balance for sediment at the low part of the tidal flat is given by the following equation:

$$\frac{\partial (A_l c_l)}{\partial t} = W_l \, w_s \left(c_{le} - c_l \right) - F_{lc} + F_{hl} \qquad \textbf{(2.7)}$$

At the high part of the tidal flat the mass-balance reads

$$\frac{\partial (A_h c_h)}{\partial t} = W_h \, w_s \left(c_{he} - c_h \right) - F_{hl} \qquad \textbf{(2.8)}$$

The exchange rate F_{hl} between the two parts of the tidal flat is formulated as

$$F_{hl} = D_h \frac{h_h}{4} \frac{c_h - c_l}{L_{hl}} \qquad \textbf{(2.9)}$$

where:

A_h	=	cross-sectional area of the high tidal flat	[m^2]
A_l	=	cross-sectional area of the low tidal flat	[m^2]
c_h	=	sediment concentration by volume in the high tidal flat part	[-]
c_{he}	=	equilibrium sediment concentration by volume in the high tidal flat part	[-]
c_{le}	=	equilibrium sediment concentration by volume in the low tidal flat part	[-]
D_h	=	diffusion coefficient of the high flats	[m^2/s]
L_{hl}	=	distance between the centre of the high flat and that of the low flat	[m]
h_h	=	effective water depth for the high tidal flat	[m]
W_h	=	width of the high part of the tidal flat	[m]
W_l	=	width of the low part of the tidal flat	[m]

The combination of Equations (2.4), (2.7) and (2.9) and taking the source terms (the right hand side of Equation (2.7)) implicit, leads to the following expression:

$$\left(A_l^n + W_l\, w_s\, \Delta t + \frac{D_l\, h_l}{L_{lc}}\, \Delta t + \frac{D_h\, h_h}{L_{hl}}\, \Delta t \right) c_l^{n+1} - \frac{D_l\, h_l}{L_{lc}}\, \Delta t\, c_c^{n+1} - \frac{D_h\, h_h}{L_{hl}}\, \Delta t\, c_h^{n+1}$$

$$=$$

$$A_l^n\, c_l^n + W_l\, w_s\, \Delta t\, c_{le} \qquad \textbf{(2.10)}$$

The combination of Equations (2.8) and (2.9) and taking the source terms (the right hand side of Equation (2.8)) implicit, leads to the following expression:

$$\left(A_h^n + W_h\, w_s\, \Delta t + \frac{D_h\, h_h}{L_{hl}}\, \Delta t \right) c_h^{n+1} - \frac{D_h\, h_h}{L_{hl}}\, \Delta t\, c_l^{n+1}$$

$$=$$

$$A_h^n\, c_h^n + W_h\, w_s\, \Delta t\, c_{he} \qquad \textbf{(2.11)}$$

The system of three linear equations ((2.5), (2.22), (2.10) and (2.11)) is now solved for the concentrations in the channel and the tidal flats.

Case B: Tidal flats are not included

In the case that tidal flats are not included, sediment transport between the low flat and the high flat and between the low flat and the channel does not take place. In fact, because the flats are not included, the concentration at the flats is not defined.

From Equation (2.3) with $F_{lc} = 0$, the following numerical equation for the concentration in the channel can be deduced:

$$c_c^{n+1} = \frac{A_c^n\, c_c^n + W_c\, w_s\, \Delta t\, c_{ce} - \dfrac{S_2 - S_1}{L}\, \Delta t}{A_c^n + W_c\, w_s\, \Delta t} \qquad \textbf{(2.12)}$$

Boundary conditions

Four types of boundary conditions can be defined by the user:

- a closed boundary
- a concentration boundary
- a transport boundary
- a dispersive transport boundary

The boundary conditions are described in the nodes.

Closed boundary

At a closed boundary, the sediment transport through the node is zero:

$$A_c\, u\, c_k - A_c\, D_c\, \frac{\partial c_c}{\partial x} = 0 \qquad (2.13)$$

Numerically, this leads to the following equation, assuming that the node is located at the beginning of a branch (if not, a similar equation holds).

$$c_k^{n+1} = \frac{D_{c,j}\, c_{c,j}^{n+1}}{0.5\, u_j\, L_j + D_{c,j}} \qquad (2.14)$$

Concentration boundary

At a concentration boundary, the concentration at the node is prescribed by the concentration which is given by the user.

Transport boundary

At a transport boundary, the sediment transport is given by the user. This leads to the following numerical equation for the concentration at the node:

$$c_k^{n+1} = \frac{A_c\, D_{c,j}\, c_{c,j}^{n+1} + 0.5\, S_k\, L_j}{0.5\, A_c\, u\, L_j + A_c\, D_{c,j}} \qquad (2.15)$$

Dispersive transport boundary

In the dispersive transport concept of van Dongeren, the sediment enters the model by dispersive transport and is proportional to the sediment demand of the system (see Van Dongeren, 1992). This sediment demand is computed by using an empirical relation with the area of the tidal flats and the total basin area as parameters. The resulting equation for the concentration at the boundary is as follows:

$$c_k^{n+1} = c_j^{n+1} + \frac{0.5\, L_j\, S_k}{A_c\, D_{c,j}} \qquad (2.16)$$

Stability criterion

In order to have an indication of the stability of the solution Method 1, such as described above, a simple analysis on the transport equation in the channel (without source terms) is performed.

$$\frac{\partial c}{\partial t} + u \frac{\partial c}{\partial x} - D_c \frac{\partial^2 c}{\partial x^2} = 0 \qquad \textbf{(2.17)}$$

After discretisation, the following equation is found:

$$\frac{c_j^{n+1} - c_j^n}{\Delta t} + u \frac{c_{j+1}^n - c_{j-1}^n}{2\Delta x} - D_c \frac{c_{j+1}^n - 2c_j^n + c_{j-1}^n}{\Delta x^2} = 0 \qquad \textbf{(2.18)}$$

The stability criterion for this equation is:

$$\frac{u^2 (\Delta t)^2}{(\Delta x)^2} \leq \frac{2 D_c \Delta t}{(\Delta x)^2} \leq 1 \qquad \textbf{(2.19)}$$

It is noted that Δx denotes the distance between the middle of a branch and the nodes, i.e. half the length of a branch.

2.3.2 Method 2: Solution of a boundary value problem

In this method, the concentration field is found by solving the steady-state equation, which is found by setting the time derivative to zero in the general sediment transport equation (see Equation (2.3)). This leads to a boundary value problem. The explicit scheme that is used (see below) makes use of the concentration in the nodes at the previous time step which can be considered as the boundary conditions of the equations for each of the branches.

Formally, this means that the time steps of nodes and branches do not match. However, by using an iteration technique, the concentration field converges to the steady-state solution.

It is noted that the time lag between the nodes and the branches (i.e. if no iteration was applied) is small on the morphological time scale, and would still be acceptable.

The structure of the iterative process is similar to the one described in Section 2.3.1.

Nodes

The concentrations in the nodes are computed in exactly the same way as the method described in Section 2.3.1, i.e. by using Equations (2.1) and (2.2).

Branches

Then the concentration in the branches is computed. Again, two cases must be distinguished:

- the branches for which sediment transport from and to the tidal flats should be included (case A)

- the branches for which no sediment transport from and to the tidal flats takes place (case B)

The user should specify the above status of the branches in the model schematization before running the ESTMORF-model.

Case A: Tidal flats included

The steady-state mass balance equation for sediment in the channel can be written by:

$$\frac{\partial A_c u c_c}{\partial x} - \frac{\partial}{\partial x}\left(A_c D_c \frac{\partial c_c}{\partial x}\right) = W_c w_s (c_{ce} - c_c) + F_{lc} \qquad \textbf{(2.20)}$$

The sediment flux from the tidal flat to the channel F_{lc} is elaborated as follows (same as Method 1):

$$F_{lc} = D_l \, h_l \, \frac{c_l - c_c}{L_{lc}} \qquad \textbf{(2.21)}$$

By the use of a central differences scheme and combining Equations (2.20) and (2.21), the following numerical expression is found:

$$\left(A_c^n \frac{D_c}{L^2} + W_c \, w_s + \frac{D_l \, h_l}{L_{lc}} \right) c_c^{m+1} - \frac{D_l \, h_l}{L_{lc}} \, c_l^{m+1}$$

$$= \qquad \textbf{(2.22)}$$

$$\left(\frac{D_c}{0.5 \, L^2} + \frac{u_1}{L} \right) A_c^n \, c_{k,1}^m + \left(\frac{D_c}{0.5 \, L^2} - \frac{u_2}{L} \right) A_c^n \, c_{k,2}^m + W_c \, w_s \, c_{ce}$$

The superscripts m and $m+1$ denote the iteration step level. The morphological time step levels are denoted by n and $n+1$.

The steady state mass balance for sediment at the low part of the tidal flat is given by the following equation:

$$W_l w_s \, (c_{le} - c_l) - F_{lc} + F_{hl} = 0 \qquad \textbf{(2.23)}$$

The sediment flux from the high tidal flat to the low tidal flat F_{hl} is elaborated as follows (same as Method 1):

$$F_{hl} = D_h \frac{h_h}{4} \frac{c_h - c_l}{L_{hl}} \qquad \textbf{(2.24)}$$

Equations (2.23) and (2.24) lead to the following numerical expression:

$$-\frac{D_l\,h_l}{L_{lc}}\,c_c^{m+1}+\left(\frac{D_l\,h_l}{L_{lc}}+W_l\,w_s+\frac{D_h\,h_h}{4\,L_{hl}}\right)c_l^{m+1}-\frac{D_h\,h_h}{4\,L_{hl}}\,c_h^{m+1}$$

$$=\qquad\qquad (2.25)$$

$$W_l\,w_s\,c_{le}$$

At the high part of the tidal flats the steady state mass balance reads

$$W_h w_s\,(c_{he}-c_h)\;-\;F_{hl}\;=\;0 \qquad (2.26)$$

Equations (2.24) and (2.26) yield:

$$-\frac{D_h\,h_h}{4\,L_{hl}}\,c_l^{m+1}+\left(W_h\,w_s+\frac{D_h\,h_h}{4\,L_{hl}}\right)c_h^{m+1}\;=\;W_h\,w_s\,c_{he} \qquad (2.27)$$

The system of three linear equations (2.22), (2.25) and (2.27) is now solved for the concentrations in the channel and the tidal flats by iteration.

Case B: Tidal flats are not included

From Equation (2.20) with $F_{lc} = 0$, the following numerical equation for the concentration in the channel can be deduced:

$$\left(A_c^n\,\frac{D_c}{L^2}+W_c\,w_s\right)c_c^{m+1}$$

$$=\qquad (2.28)$$

$$\left(\frac{D_c}{0.5\,L^2}+\frac{u_1}{L}\right)A_c^n\,c_{k,1}^m+\left(\frac{D_c}{0.5\,L^2}-\frac{u_2}{L}\right)A_c^n\,c_{k,2}^m+W_c\,w_s\,c_{ce}$$

This equation is solved for c_c by iteration.

Boundary conditions

The implementation of the boundary conditions is exactly the same as that of Method 1.

Stability criterion

In order to have an indication of the stability of the solution Method 2, such as described above, a simple analysis on the transport equation in the channel (without source terms) is performed.

In simplified form, Equation (2.20) reads:

$$u \frac{\partial c}{\partial x} - D_c \frac{\partial^2 c}{\partial x^2} = 0 \qquad \textbf{(2.29)}$$

After discretisation, the following equation is found:

$$u \frac{c_{j+1}^n - c_{j-1}^n}{2\Delta x} - D_c \frac{c_{j+1}^n - 2c_j^{n+1} + c_{j-1}^n}{\Delta x^2} = 0 \qquad \textbf{(2.30)}$$

The stability criterion for this equation is:

$$\frac{u \Delta x}{D_c} \leq 2 \qquad \textbf{(2.31)}$$

It is noted that Δx denotes the distance between the middle of a branch and the nodes, i.e. half the length of a branch.

2.3.3 The cross-sectional area

The change of the cross-sectional areas of the channel, the low tidal flats and the high tidal flats satisfy the following equations:

$$\frac{\partial A_c}{\partial t} = W_c \, w_s \, (c_{ce} - c_c) \qquad \textbf{(3.1)}$$

$$\frac{\partial A_l}{\partial t} = W_l \, w_s \, (c_{le} - c_l) \qquad \textbf{(3.2)}$$

$$\frac{\partial A_h}{\partial t} = W_h \, w_s \, (c_{he} - c_h) \qquad \textbf{(3.3)}$$

Using Euler's method yields the following numerical relations:

$$A_c^{n+1} = A_c^n + \Delta t \, W_c \, w_s \left(c_{ce} - c_c^{n+1}\right) \qquad \textbf{(3.4)}$$

$$A_l^{n+1} = A_l^n + \Delta t \, W_l \, w_s \left(c_{le} - c_l^{n+1}\right) \qquad \textbf{(3.5)}$$

$$A_h^{n+1} = A_h^n + \Delta t \; W_h \; w_s \left(c_{he} - c_h^{n+1}\right) \tag{3.6}$$

Remarks:
1. The sediment concentration at the new time step (with superscript $n+1$) is already computed, using the formulae described in Section 2.3.2.
2. For the case that the tidal flats are not included (case B, see Section 2.3.2), Equations (3.2), (3.3), (3.5) and (3.6) are not used.

3 Testing programme

3.1 Introduction

In this chapter, the tests that have been performed during Phase II are described. During Phase I, debugging tests, first prototype tests and real model tests have already been done. Phase II tests comprise a brief sensitivity analysis for prototypes in order to get a feeling for the values of the parameters (see Section 3.2) and prototype tests for sea level rise (Section 3.3) and land subsidence (Section 3.4). Finally, in Section 3.5, an brief overview of the results of a test with respect to the nodal point relations is presented.

It is evident that debugging tests and prototype tests have been performed to check new implemented modules and changes made to the existing modules.

3.2 Sensitivity analysis

The purpose of the sensitivity analysis is to get a feeling of the effect of (changing) the values of parameters on the results of the simulations. In order to keep the results well-comparable, these tests have been performed on a simple prototype: a semi-closed tidal basin without flats.

This prototype consists of a channel, which is open at one end and closed at the other end. At the open boundary, the tidal level is prescribed.

The initial geometry of this prototype is characterised as follows:

length of the basin	:	15000 m
width of the channel	:	1000 m
depth of the channel (below MSL)	:	10 m
amplitude of the tide	:	1 m

The model consists of 15 branches, each with a length of 1000 m.

The sensitivity analysis has been done on the following parameters:
- fall velocity
- equilibrium concentration
- dispersion coefficients
- power of the equilibrium relations (see Karssen and Wang, 1993).

These parameters have been selected because of their impact on the time scale of the morphological change and on the spatial distribution of the sediment.

First, a basis condition has been chosen. In view of the fact that it concerns a sensitivity analysis, it is not very important what combination will be used as a basis; the analysis will be on the impact of **changes** of the relevant parameters on the results. In Table 3.2.1 below the combinations of parameters that have been used in the sensitivity analysis are listed.

Run-id	D_c [m^2/s]	W_s [m/s]	C_E [-]	n_{MSL} [-] [1]
000	10	0.001	0.001	4
011	10	0.0001	0.001	4
012	10	0.01	0.001	4
021	1	0.001	0.001	4
022	100	0.001	0.001	4
031	10	0.001	0.0001	4
032	10	0.001	0.01	4
041	10	0.001	0.001	3
042	10	0.001	0.001	5
045	10	0.001	0.001	2
046	10	0.001	0.001	1

Table 3.2.1 Combination of parameters used for the sensitivity analysis

Figures 3.2.1 through 3.2.11 show the time series of bed levels during the above simulations with intervals depending on the speed of the changes. These intervals vary between 5 years and 75 years.

The time step of the simulations is one month, whereas the simulation time equals 3600 timesteps, i.e. 300 years.

The results show that for the basis situation, the basin fills up from the open sea boundary. After 300 years, the basin is almost completely filled up. The results can be summarized as follows:

- The impact of a change of the fall velocity (Runs 011 and 012) is that a larger fall velocity leads to more deposition near the open boundary at the start of the computation, whereas with a smaller fall velocity more sediment is deposited at the back of the estuary. The shape of the bed along the basin is convex.
- The impact of a change of the dispersion coefficient (Runs 021 and 022) is that a larger dispersion coefficient leads to more (diffusive) transport to the back of the estuary (from locations with high to locations with low concentrations) and the estuary will fill up rapidly. Similarly, a smaller diffusion coefficient results in less rapid deposition. The shape of the bed along the basin is convex.
- The impact of a change of the equilibrium concentration (Runs 031 and 032) is that a larger concentration leads to rapid siltation, and a small concentration results in smaller siltation rates.

[1] see Karssen and Wang (1993)

The basin fills up from the open boundary side. The shape of the bed along the basin is convex.

- The impact of a change of the power of the equilibrium relation (Runs 041, 042, 045 and 046) is that small values (1 and 2) lead to siltation at the back of the basin first, and the bed has a concave shape. For a power equal to 2, the distribution of the deposition is almost uniform over the basin. For higher powers, deposition first occurs near the open boundary, and the bed has a convex shape.

Note: For a sensitivity analysis, it may be quite useful to assess the results for a whole range of parameters. However, some of these parameter values may not be realistic. This is especially the case for the power of the equilibrium relation.

The above gives an indication of the impact of changes in parameter values on the results if applied on non-prototype models, such as the Westerschelde model and the Friesche Zeegat model.

3.3 Sea level rise

One of the requirements of the ESTMORF model is the capability to simulate the morphological behaviour of estuaries due to the impact of sea level rise (Karssen and Wang, 1992). The sea level rise is in the order of about 100 cm per century, although considerable variations in the estimates for the rates is found in literature.

For the ESTMORF model, a change in mean sea level means a change in the mean water level such as prescribed at the sea boundaries. The subsequent change in the hydrodynamics should then lead to a new morphological equilibrium and thus to morphological changes in the model.

The change in mean sea level per morphological time step can be given by the user in one of the input files (see User Manual). By doing so, the existing boundary conditions for the hydrodynamic computations are adapted automatically through a change in mean sea level before every hydrodynamic computation. The interval of the hydrodynamic computation is also prescribed by the user.

The definition of what is considered to be part of the channel and part of the tidal flats, as well as the equilibrium relations for the heights of the tidal flats depends on the water levels. A sea level rise will lead to a change in these values. The exact impact on the water levels will vary from estuary to estuary (or model to model).

A simple test has been performed to determine whether the sea level rise is implemented correctly in ESTMORF by studying the resulting ESTMORF-profiles and the hydrodynamic output in the prototype model of a tidal basin without tidal flats (see Section 3.2).
A sea level rise of 1 cm per month was prescribed, which is unrealistic, but makes comparison and analysis of the results easier.

The results are summarized in Table 3.3.1 below. The table shows that the maximum and minimum water levels increase with 1 cm per year, and so did the points in the profile separating the channel part from the low tidal flats and the low tidal flats from the high tidal flats.

level	t = 0 months		t = 6 months		t = 12 months	
	x [m]	y [m]	x [m]	y [m]	x [m]	y [m]
MHW	492.32	1.02	493.12	1.07	494.08	1.13
width and height of high flats	450.48	0.46	455.00	0.49	460.09	0.53
MSL	398.62	0.01	404.41	0.06	411.42	0.12
width and height of low flats	324.70	-0.47	331.52	-0.45	340.07	-0.42
MLW	260.40	-1.02	260.41	-0.97	260.42	-0.91
channel bed	260.40	-9.65	260.40	-9.65	260.40	-9.65

Table 3.3.1 Change in widths and heights of the profile at the end of the basin due to sea level rise. x- and y-coordinates denote the distance from the centre axis and the original Mean Sea Level, respectively.

It is concluded that the impact of sea level rise is implemented properly.

3.4 Land subsidence

Land subsidence means that the earth surface is subsiding due to human interference. In The Netherlands, land subsidence is mainly caused by gas mining, of which the impact is most pronounced in the Wadden Sea.

For the model, the impact of land subsidence is that the bed level decreases for all points of the cross-sectional profile.

At this moment, a global land subsidence can be given by the user. However, for future applications, it may be necessary to prescribe a space-varying land subsidence; land subsidence is a more local phenomenon than sea level rise. In view of this, the memory allocations of ESTMORF are already set up in such a way that this feature can be used in the future by a very simple change in the software.

The software has been tested with a prototype including tidal flats and a land subsidence rate of 10 cm per month, which is, again, not realistic but such a value makes testing more easy. Figure 3.4.1 shows the cross-sectional profiles at the closed end of the basin (where the changes due to sediment input is the smallest at the start of the computation) for the start of the simulation, and after 4, 8 and 12 months.

The graphs show that the channel bed lowers with 10 cm per month (checked in the output files). In view of the fact that the water levels remain relatively unchanged, the channel profile area increases, whereas the width of the high flats decreases. This leads to increasing widths of the low flats and a smaller slope over the main part of the low flats. The total width of the branch remains unchanged, which results in steep high flats.

The above development is in line with the expectations. It is concluded that the impact of land subsidence is correctly implemented.

3.5 Nodal point relations

In the framework of EENDMORF, the nodal point relations with respect to the distribution of sediment at a bifurcation are studied. This was done by morphodynamic simulations with a simple geometry consisting of one river branch, bifurcating into two tidal channels near the sea. It was concluded that, starting from a situation with two open tidal channels of equal depth, a small disturbance from this situation leads to the closure of one of the two channels (Wang et al., 1993).

In view of the fact that a similar nodal point relation is used in ESTMORF, a simple test has been performed for the situation described above.

The results show that one of the branches closes. This is easy to explain: if the discharge (or tidal volume) through the shallow channel decreases, it on its turn decreases the equilibrium cross-sectional area, etc.

The impact of the above on complex models, such as the Friesche Zeegat and the Westerschelde, is not clear. It should however be noted that such an impact may exist, and it may be necessary to implement another form of the nodal point relation in ESTMORF. It is recommended not to start an implementation before completion of the study of these relations in the framework of EENDMORF.

4 The Westerschelde model

4.1 Introduction

This chapter presents the set up, calibration and validation of the Westerschelde model. Section 4.2 describes the model in its initial state (1968 geometry), whereas Section 4.3 gives an overview of the calibration and validation data such as provided by Rijkswaterstaat.

4.2 Description of the model

model geometry

The ESTMORF Westerschelde model is based on the IMPLIC/DUFLOW Westerschelde model, using a schematization of the geometry dating from 1968, such as provided by Rijkswaterstaat. In order to simulate the morphological behaviour using ESTMORF, the equilibrium relations should be known. These relations can be determined by computing the coefficients in the relations from available data on the geometry and hydrodynamic conditions in a situation which is considered to be an equilibrium situation for the area under consideration.

It is agreed with the client that the geometry of the Westerschelde before the deepening in the years 1970-1980 can be considered as a sort of equilibrium situation. The existing IMPLIC model schematization of 1968 then well serves as a model representation of this 'equilibrium' situation. One should note that this is an approximation; during the years 1965-1970, the eastern part of the Westerschelde is characterized by a considerable human interference leading to decreasing and increasing cross-sectional areas of the channels (Jeuken, 1993). The impact of this interference in the years 1965-1970 can, however, be considered small compared to the large dredging activities in the years 1970-1980, making the choice for this geometry to be an equilibrium condition justified.

The model consists of 180 normal branches, simulating the channel/flat system, and 10 weir branches, simulating the short-cut channels over tidal flats, that exist during high water conditions. Figure 4.2.1 shows the branches of the 1968 model in the 1971/72 bathymetric chart. The branch/node system is presented in Figure 4.2.2. It is clear that the model consists of a large part in the Westerschelde, but also of a part in Belgium, representing the rivers Schelde, Rupel, Durme, Dender, Zenne, Dijle and Nete.

At the start of ESTMORF-simulations, the IMPLIC-schematization, consisting of cross-sections described by 20 points, is transferred into an ESTMORF-schematization, consisting of a cross-sections described by 7 points. This transformation is done using the relations which describe the cross-sectional profile, such as worked out in Karssen and Wang (1993). It appeared that there are many channels in the Westerschelde model of which the profile doesn't meet the requirements such as laid down in the relations. For example, channels with vertical 'walls' (so no flats) and channels with partly vertical walls are found in the model. Special adaptations to the relations and transport equations were worked out and implemented during Phase I and II of the project, see also Karssen (1994).

boundary conditions

ESTMORF makes use of two types of boundary conditions: those for the hydrodynamic computations and those for the morphological computations. The boundary conditions for the morphological computations are calibration 'parameters', and are therefore not fixed.

The boundary conditions for the hydrodynamic computations were determined by Rijkswaterstaat during the calibration of the IMPLIC Westerschelde model, and should remain fixed during the process of calibration of the (ESTMORF) morphological model. This brings up a problem: the model makes use of residual currents which should be computed over a cyclic period[2]. The choice of a proper cyclic tide or tidal period which is characteristic for morphological changes has not yet been determined, although basic research is going on at several institutes in the world.
It was decided to select a period from the boundary conditions provided by Rijkswaterstaat of approximately 12.5 hours duration, viz the period from 11 May 1971 8:40 to 12 May 1971 21:00, which was about an average tide and make these cyclic. It is recommended to investigate the impact of a change in the hydrodynamic boundary conditions on the morphological changes in further studies.

The upstream boundary conditions were also provided by Rijkswaterstaat, and are listed in Table 4.2.1 below. During the simulations, problems occurred in the boundary condition of river Zenne. In view of the small discharge, it was decided to close that boundary, which immediately solved the problem.

Boundary	Discharge [m^3/s]
Schelde	3
Nete	7
Dijle	13
Zenne	6 -> 0
Durme	0
Dender	0

Table 4.2.1 Discharge boundary conditions such as prescribed in the Westerschelde model

The morphological boundary conditions should be prescribed at all open boundaries of the model.

[2] The length of this period is determined by the length of the prescribed cyclic boundary time series; this time series is repeated during the whole simulation. ESTMORF automatically computes the ebb and flood volumes over this cyclic period, which on their turn determine the residual currents and the equilibrium parameters for the geometry.

Three quantities can be prescribed at the boundaries: the concentration, the transport or the diffusive transport (Van Dongeren, 1992). Although tests have been performed to check the implementation of the boundary conditions, in view of simplicity and the fact that the general behaviour of the model was to be studied, it was decided to do the calibration using concentration boundaries only. The values for the concentrations are calibration parameters.

4.3 Calibration and validation data

4.3.1 Available data

human interference

In order to simulate the morphological behaviour of the Westerschelde between 1968 and 1990, the human interference in that period should be known. Rijkswaterstaat provided data on floppy disk of the dredging and dumping activities in the form of dredged and dumped volumes in each of the branches of the model for each month in the period 1965-1993.

volumes

During the calibration, new measurement data became available on the 'wet' volumes of six areas in the Westerschelde, see Figure 4.3.1. In order to make a proper comparison and avoid making use of deviations that are already present in the initial state, the measurement data are transferred to relative volumes with respect to the 1968 volumes first.

cross-sectional areas

Table 1 of Svasek (1994) lists the cross-sectional area below NAP of 12 discharge sections. Each discharge section consists of two or more cross-sections in the model. For calibration purposes, the cross-sectional areas of the model should thus be summed.

The cross-sectional areas of separate channels are listed in Appendix 1 of Svasek (1994).

deposition and erosion charts

Jeuken (1993) contains bathymetric charts of the Westerschelde for the years 1965, 1970, 1975, 1980, 1985 and 1990, and maps showing the differences between the consecutive bathymetries of those years.

4.3.2 Consistency of the data

During the calibration procedure, it became clear that not all of the various calibration data are mutually consistent (see Section 4.4).

In their report, Van den Berg et al (1991) defined 13 areas for which the volumes of human interference during 5 years periods between 1965 and 1985 have been worked out. Hence, the summation of the branch data provided by Rijkswaterstaat over the branches in these 13 areas over the relevant years should equal these area data. Table 4.3.1 below shows the result of the intercomparison for the years 1970-1975 and 1975-1980 (the years in the calibration period). The summation of the branch data was done by a software program.

Area	volume of human interference (10^6 m^3)			
	1970-1975		1975-1980	
	summation of branch data	area data	summation of branch data	area data
1	-9.7	-8.8	-13.5	-11.6
2	6.4	5.6	0.9	0.3
3	-0.3	-0.1	4.7	4.0
4	-2.2	-1.9	-6.7	-6.7
5	-6.4	-5.7	-6.4	-5.1
6	-0.2	0	-0.3	0.2
7	-7.2	0.1	-2.0	0.3
8	2.9	-0.6	10.5	8.3
9	3.8	2.0	5.6	5.4
10	-5.0	-4.2	-4.3	-3.4
11	-1.1	-0.2	-2.5	-1.3
12	-2.8	-5.6	-3.3	-4.7
13	-1.5	-1.4	-5.2	-3.4
Total	-23.3	-20.8	-22.5	-17.7

Table 4.3.1 Comparison of volumes of human interference computed by summation of branch data and data per branch (negative = dredging, positive = dumping)

Table 4.3.1 shows that the total volume of human interference in the years 1970-1975 differ between both methods. For 1970-1975 the difference is in the order of 10%, whereas for 1975-1980 the difference is in the order of 25%. It is also remarkable that most areas compare reasonably well for both methods, while the areas 7, 8 and 12 show large differences. Especially in the period 1970-1975, the differences for area 7 are very large.

Although the volumes of human interference are of course no calibration data, they are important input for the simulations and their quality determines the reproduction of the model.

From information provided by Rijkswaterstaat, it became clear that the data on the volumes of human interference *per branch* are most probably more reliable than those of the *area* volumes. Part of the differences might be due to the method of subdivision of the Westerschelde into the 13 (or 21) areas which is not completely equal in both datasets. It is concluded that the volumes of net deposition and erosion in the areas have to be viewed with certain distrust.

A similar comparison was made for the cross-sectional areas in Svasek (1994). It appeared that the summation of the cross-sectional areas of the separate branches in a discharge section, such as listed in the Appendix 1 of Svasek (1994), is in general not equal to the cross-sectional areas of the discharge sections, such as listed in Table 1 of Svasek (1994). From information of the Rijkswaterstaat, the reason became clear. The separate cross-sectional areas are measured perpendicular to the branch axis, whereas the discharge sections are often far from perpendicular, leading to a systematical overestimate of the cross-sectional area. The cross-sectional areas of the separate branches are therefore more reliable.
It is noted that the separate branches do not always lie exactly on the discharge sections, which may also cause deviations.

4.3.3 Conclusions

In the previous sections the available data is analyzed. Some inconsistencies exist in the available data, which has led to the following conclusions with respect of the use of the data for calibration and validation purposes:

- The volumes of human interference (dredging and dumping) such as provided by Rijkswaterstaat on floppy disk should be used to incorporate the human impact on the bed levels in the Westerschelde in the model.
- The cross-sectional areas for the separate branches such as listed in Appendix 1 of Svasek (1994) are the best quantitative data to calibrate and validate with. In view of the fact that data are only available for the years 1960/61, 1977/78 and 1992 and the model schematization is available in 1968, the calibration and validation period of the model should be combined. The calibration (validation) period will then be 1968-1992 (25 years).
- The volume data such as provided by Rijkswaterstaat are very well suitable to calibrate with quantitatively.
- The bathymetric charts in Jeuken (1993) can be used during the calibration and validation as a method to compare the computed net behaviour in the channels with field data in a qualitative way.

The above conclusions can be summarized as follows: the calibration should purely be done on geometrical data (cross-sectional areas and volumes) and the qualitative morphological behaviour (erosion, deposition) of the channels. This conclusion is based on the availability and the practical use for calibration purposes of the data.

Notes: 1. The quality of the data provided is the best available. The various methods of how the data is obtained have led to inconsistencies and the above conclusions.
2. The amount of morphological data that is available of the Westerschelde is well above the amount of data that is generally available in estuaries.

4.4 Calibration and validation

set-up and rough calibration

First, the model was set up and several test runs were performed to have an indication of the properties of the model. During that phase, channels/branches with (partially) vertical walls were detected and marked as such in the model schematization file (see also User Manual).

Further, a rough idea of the ranges for the calibration parameters was formed by changing the relevant parameters considerably. The following parameters have been used as calibration parameters:

- dispersion coefficient for the channel transport,
- fall velocity, and
- equilibrium concentration.

The dispersion coefficient for the transport between the flats and the adjacent channel, and the dispersion coefficient for the transport between the low and high flats have not been changed after the first rough calibration runs. This has two reasons: the impact was rather small and, most important, the form of the empirical relations for the flats such as used in the model, were deduced for the Wadden Sea area. The model results with respect to the height of the flats in the Westerschelde are therefore considered to be non-reliable. They need separate calibration.

During the rough calibration, it became clear that some branches silted up due to the human interference, while they were not supposed to. The reason is that, in the model, the sediment is dumped in the channel part only, which is not in accordance with reality, where disposal takes place on the edges of the flats and sometimes only during certain phases of the tide. The idea behind this is that a minimal amount of the disposed sediment will return into the (shipping) channels, keeping the channels open.

This feature was detected first in the disposal of sediment on the Land van Saeftinghe (Branch 95 of the model). In consultation with Rijkswaterstaat it was decided to divide these dumped volumes over the Branches 94 and 96. During calibration runs including the period 1980-1992, the Branches 94 and 96 showed a similar behaviour as Branch 95. To get the model going, the disposal in the Channels 93, 94, 95 and 96 were removed from the human interference file.

detailed calibration

Changes in the fall velocity and the equilibrium concentration have a similar impact on the results of the simulations (see also Section 3.2). Therefore, one of these parameters can remain constant during the calibration. Based on information provided by Rijkswaterstaat, the fall velocity in the Westerschelde on average is 2 cm/s, which is the value used in the detailed calibration runs.

Note: The fall velocity in the model is not necessarily the same as the fall velocity in the field, and the choice of this value is purely justified from the point of view that the calibration will be done with the equilibrium concentration as calibration parameter.

Table 4.4.1 below lists a summary of the detailed calibration runs which are performed. For all runs at least a simulation was performed of 12 years (1968-1980), for the Runs 1, 6 and 9 a simulation of 25 years was made (1968-1993).

Run	c_E [-]	D_c [m^2/s]	res. curr. parameter [-]
1 (100)	0.000001	100	0.5
2	0.000001	**50**	0.5
3	**0.0000001**	100	0.5
4	**0.0000005**	100	0.5
5	0.000001	100	**0.**
6 (110)	**0.00001**	100	0.5
7	**0.000005**	100	0.5
8	**0.000003**	100	0.5
9 (300)	0.000001	**500**	0.5

Table 4.4.1 Overview of calibration runs of the Westerschelde model (not complete). Fat numbers denote the calibration parameter for that run. The residual current parameter is a multiplication factor on the residual current to take into account the non-uniform distribution of sediment over depth.

The results of most of the runs showed either a behaviour that was very similar to one of the Runs 1, 6 and 9, or led to almost no morphological changes. Therefore, only three runs are worked out in this report in more detail: Runs 1, 6 and 9 of the above table, with run identification numbers 100, 110 and 300, respectively.

An interesting, but - from a software implementation point of view - complicating, feature was found: some channels filled up during the computations. As a result, the computation stopped. This is logical: when the bed level in the channel rises above the low water level, the requirements of the ESTMORF-profile (Karssen and Wang, 1993) cannot be met. Due to the termination of the computation after filling up of a channel, the total calibration period could not be simulated in one single run. As a consequence, special procedures and software programs have been developed to restart a computation. The restart procedure includes the necessary removal of the branches that have silted up from the model schematization, the file with empirical relations and the human interference file.

The filling of channels provides a check on the calibration. The silted channels are summarized in Table 4.4.2 for the three Runs 100, 110 and 300. In the table the year of total filling up of branches for each of these runs is listed.

Runid	Branch number (location see Figure 4.2.1)								
	27	82	83	84	85	86	104	105	110
100		1980							
110	1989	1971	1974	1974	1971	1974	1991	1973	1987
300		1973	1986	1992	1992	1992		1977	

Table 4.4.2 Year of total filling up of branches for the Runs 100, 110 and 300

Table 4.4.2 shows that one of the channels fills up for all simulations, i.e. Branch 82, which is one of the channels crossing the Platen van Valkenisse. A comparison with charts in Jeuken (1993) learns that this channel has indeed filled up during the years 1970-1980. For the three runs with id 100, 110 and 300, the total filling of Channel 82 occurred in 1980, 1971 and 1973, respectively. From the available information, it is difficult to determine the exact year of complete filling up. It is estimated that the runs with id 110 and 300 are most likely better in timing than run with id 100.

A similar reasoning goes for the Channels 83 through 86 (channels crossing the Platen van Valkenisse), which have also filled up in the years 1971 - 1974 for Simulation 110 and in 1986 - 1992 for Simulation 300. Comparison with the charts of Jeuken (1993) leads to the conclusion that the timing of Simulation 300 is better than the other simulations. Further, an important conclusion is that the model simulates the development of the Platen van Valkenisse properly.

Note: Branch 86 is a structure branch, which had to be removed after the removal of the Branches 83 and 84 to prevent having a structure branch as a closed end of the network.

Branch 27 (the Thomaes Channel) fills up in Simulation 110, which is strange: according to the available information, this channel still exists in 1992 and has remained approximately unchanged or has even deepened somewhat (van den Berg et al, 1991).

The filling up of the Branches 104 and 105 on the Plaat van Saeftinghe is not according to the observations. In fact, the level of these flats has decreased. An explanation of this incorrect behaviour might be the incorrect form of the equilibrium relations for the tidal flats in the Westerschelde model.

Another way to check the calibration is to compare the cross-sections of the channels. As was already concluded in Section 4.3.3, the cross-sectional areas in the years 1977/78 and 1992 could best be used for the calibration. Therefore, these areas have been compared for the Runs 100, 110 and 300.

Two methods for comparison of the cross-sectional area information are applied:

- a comparison of the computed and observed absolute areas in the years 1977/78 and 1992, and
- a comparison of the computed and observed relative area change between 1977/78 and 1992.

Besides that the first method directly gives a comparison between the cross-sectional areas as a result of 9-10 years of simulation (1968-1977/78), and of 25 years of simulation (1968 - 1993) and the measured cross-sectional areas in these years on one hand, this method on the other hand also indicates whether the measured cross-sectional areas are comparable to the cross-sectional areas in the model anyway. The latter is explained later.

In the second method, the relative (area) change between 1977/78 and 1992 is defined as follows:

$$\Delta A_r = \frac{A^{1977/78} - A^{1992}}{A^{1977/78}} \qquad \textbf{(4.1)}$$

where:

ΔA_r	=	relative area change	[-]
$A^{1977/78}$	=	cross-sectional area in 1977/78	[m^2]
A^{1992}	=	cross-sectional area in 1992	[m^2]

The above formula is defined such that a negative value represents enlargement of the area, whereas a positive value represent a decrease of the area, which is consistent with the notations found in the available literature.

Figures 4.4.1 - 4.4.3 present the relative area changes and the absolute areas in 1977/78 and 1992, for the Runs 100, 110 and 300, respectively.

The graphs of the relative areas show the computed relative change plotted against the observed relative change for a number of selected channels branches in the model. These branches were selected on three criteria:

- The Westerschelde area should be well-covered.
- The Westerschelde area should be well-represented.
- Measurement data should be available at approximately the centre of the branch for the years 1977/78 and 1992.

A perfect model would lead to graphs with all points on the 'y = x curve', because in that case model and observations are the same. The relative area change graphs also indicate whether the behaviour of the model is correct: a point in the upper right quadrant denotes deposition for both the model and observations, whereas a point in the lower left quadrant denoted erosion for both the model and observations. The other quadrants indicate an opposite behaviour.

The graphs indicate that the impact of the changes of the parameter values for the equilibrium concentration and the dispersion do not change the results much.

In the upper graphs of Figures 4.4.1 - 4.4.3, the comparison of computed and observed relative change of the cross-sectional areas is given. A cloud of points is found around 0, which is an indication that most of the areas do not change much both in the model and in nature. These small changes show however that the tendency of the model is not always correct: some points are found in the upper left quadrant, which shows that the model predicts erosion, whereas in nature deposition is found. The general trend, however, is that the points remain reasonably around the y = x axis.

Some large differences are still occurring in the Branches 61, 74, 98 and 100, representing parts of the Overloop van Hansweert, Schaar van Waarde, Overloop van Valkenisse and Nauw van Bath. The cross-sectional areas in these branches in 1977/78 and 1992 are listed in Table 4.4.3 below for the Runs 100, 110 and 300, and the observations.

Branch number	Area in 1977/78 [m^2]				Area in 1992 [m^2]			
	Observed	Model			Observed	Model		
		100	110	300		100	110	300
61	20333	26106	25529	25234	22959	25717	18671	17830
74	12509	12014	11074	11217	15368	8817	8022	7891
98	13419	12538	12298	11968	15324	21647	19633	20523
100	8563	8868	10308	9449	9200	10179	15947	13114

Table 4.4.3 Cross-sectional areas of branches with large deviations between model and observations

For Branch 61, the area in 1977/78 is already incorrect, which may well be due to a difference in the location and length of the cross-section. The deviations in Branch 74 are easy to explain: large quantities of dredged material have been dumped in this branch during the years 1965-1992, which is included in the model by dumping in the channel part. In reality, however, this material is dumped on the flats, and will not all return into the channel easily. This property of the model and a proper method to deal with this type of dumping in the software, should be investigated in later studies. The qualitative behaviour in the Branches 98 and 100 (erosion) is simulated properly, but the process of erosion is too strong.

The two lower graphs of Figures 4.4.1 - 4.4.3 make clear that the behaviour of the model in the period 1968 - 1977/78 is reasonably good for all three simulations. The results for 1992, however, also indicate that the deviations from the observations - on average - increase in time.

The results of the calibration runs are also compared with volumetric data for six areas (see Figure 4.3.1) over the years 1968 - 1993. Time series of the computed and measured volumes of these six areas (relative to the 1968 volume) are presented in Figures 4.4.4 and 4.4.5 for Run 100, whereas Figures 4.4.6 and 4.4.7 present the similar graphs for Run 300.

The graphs show that both for Run 100 and 300, the computed volumetric changes in the

Areas 4 - 6 are in good agreement with measurements. It should be noted that the changes in these areas are small. For Areas 1 - 3, the results of Run 300 are better than those for Run 100. Area 3 is for Run 300 in good agreement with measurements, but although there is a clear improvement, the results for Areas 1 and 2 are still off for both runs. In view of the improvement, it may be that a space-varying dispersion coefficient (high values in Areas 1 and 2) may improve the results further. Another explanation may be that no sediment is disposed in these areas in the model, whereas this occurs in practice. A shift of the disposed volumes from the Land van Saeftinghe to the area around Bath may also help to solve this problem, which has been studied in an additional simulation (see below).

The above information gives an indication of the development of the Westerschelde model by means of quantitative results. Figures 4.4.8 and 4.4.9 give a graphical representation of the cross-sectional profiles near the entrance of the Westerschelde (Branches 1, 11 and 19) and near Valkenisse (Branches 76, 82, 91), respectively. The profiles indicate that the development near the entrance is slow and very small. Almost no differences are found between the 1968 and 1993 profiles. Near Valkenisse, the development is much more pronounced. The Schaer van Waarde is shallowing, whereas the small channel crossing the Plaat van Walsoorden has filled up completely during the simulation (see also Table 4.4.2). In the model this is found by a rise of the bed level above MLW. The lower graph of Figure 4.4.9 shows two bed levels for the centre channel (Branch 82). The solid line represents the level at which the channel is removed from the model. In the simulation period after this removal, the geometry is then effectively such as represented by the dashed line.

additional simulation

The results of the calibration of the Westerschelde model, as described above, have given rise to a further evaluation of the ESTMORF program and its application to the Westerschelde case. Such an evaluation has been done in the beginning of 1995.

As a result, a new simulation has been performed with the Westerschelde model, including a shift of the dumping and dredging volumes from the Land van Saeftinghe to the area near Bath, following the above mentioned recommendation. The volumetric results of this simulation (Runid 500) compare much better than previous runs, see Figures 4.4.10 and 4.4.11.

The new simulation run differs in two respects from the simulation with Runid 300:

- In view of the previously mentioned rapid recirculation of sediment between the dump area 'het Land van Saeftinghe' (branche 95 of the Westerschelde model) and the dredging area 'het Nauw van Bath', the sediment of het Nauw van Bath is not dumped in Saeftinghe but returned to Bath with a retardation of 3 months.
- The part of the program handling the dumping of sediment is improved.

For a more elaborate description of this evaluation and the obtained results, see Karssen (1995).

4.5 Conclusions

The Westerschelde model has been set up and a first calibration has been performed.

The calibration data has been verified on mutual inconsistencies, which has led to restriction of the calibration data to cross-sectional areas and visual inspection of the proper behaviour with respect to deposition and erosion. The calibration and validation period has been combined, because measured cross-sectional area data for comparison is available for the years 1977/78 and 1992 only.

The final calibration runs show that the filling up of a number of channels in the eastern Westerschelde is simulated properly, indicating that the development of the Platen van Valkenisse is well predicted by the model.

The relative cross-sectional changes between 1977/78 and 1992 are in reasonable agreement with observations, but the results are certainly not perfect.

The agreement of the computed and observed volumetric changes varies over the Westerschelde area. Near the mouth of the Westerschelde up to Hansweert, the model results compare very well with the measured volumes. It is noted that the volumetric changes in this area are small. In the area east of Hansweert, the comparison is somewhat worse, although the tendency is correct. A shift of the dumping and dredging volumes from the Land van Saeftinghe to the area near Bath in combination with a dispersion coefficient of 500 m^2/s, such as performed in the framework of an additional evaluation (Karssen, 1995), has led to a considerable improvement of the model results in that area.

The form of the empirical relations for the tidal flats in the Westerschelde model are copied from those for the Wadden Sea. This may lead to an incorrect model behaviour.

The impact of the hydrodynamic boundary conditions on the results is not clear. A 12.5 hours cyclic period has been selected from data provided, but in how far other boundary conditions would have affected the results is not studied.

5 The Friesche Zeegat

5.1 Introduction

The Friesche Zeegat is a tidal inlet system located in the North-east of the Wadden Sea. The inlet of the basin is located between the islands Ameland and Schiermonnikoog, see Figure 5.1.1, representing the bathymetry of the Friesche Zeegat in 1957, i.e. before the closure of the Lauwerszee.

From a morphological point of view, the Friesche Zeegat is one of the most interesting tidal basins of the Wadden Sea. In 1969, a part of the channel system has been cut off by the closure of the Lauwerszee, see the bathymetric chart of 1985 depicted in Figure 5.1.2. This human interference has reduced the backbarrier area with about 91 km^2 leading to a reduction of the tidal prism (= half of the tidal volume) from 305 million m^3 to 200 million m^3 (i.e. a reduction of about one third). (Biegel, 1991)

This major human interference has resulted in morphological changes that are still going on; deposition is occurring in most of the channels in the Friesche Zeegat. The aim of the ESTMORF Friesche Zeegat model is to show that this model is well-capable to simulate these morphological changes. As these changes are still going on, positive results may lead to the conclusion that the model can be used for predictive purposes.

This chapter presents the calibration and validation of the Friesche Zeegat model. First, a description of the model is given in Section 5.2. Then, Section 5.3 contains an overview of the data used for the calibration and validation. The calibration and validation can be found in Section 5.4, whereas the conclusions are drawn up in Section 5.6.

5.2 Description of the model

model geometry

The ESTMORF Friesche Zeegat model is based on the IMPLIC/DUFLOW Friesche Zeegat model, with a geometry (schematization) dating from 1958, i.e. well before the closure of the Lauwerszee in 1969. The model was provided by Rijkswaterstaat. In order to simulate the morphological behaviour using ESTMORF, the equilibrium relations should be known. These relations are determined by computing the coefficients in the relations from available data on the geometry and hydrodynamic conditions in a situation which is considered to be an equilibrium situation for the area under consideration. This situation is before the closure.

The model before closure consists of 133 normal branches, simulating the channel/flat system. Figure 5.2.1 shows the location of the channels of the 1958 model. The branch numbers are presented in Figure 5.2.2. The model consists of the inlet, ebb tidal delta and backbarrier system of the Friesche Zeegat, which includes the Pinkegat, Smeriggat, Zoutkamperlaag and Gat van Schiermonnikoog. In the situation before closure, the model also contains the Lauwerszee. (See Figure 5.1.1).

The model after closure consists of 87 branches, see Figure 5.2.2. The closure of the Lauwerszee is just north of the line consisting of the Branches 88 to 92.

boundary conditions

The boundary conditions for the hydrodynamic computations were determined by Rijkswaterstaat during the calibration of the DUFLOW Friesche Zeegat, and have remained fixed during the process of calibration of the (ESTMORF) morphological model. The open boundaries are located at the ends of the Branches 61, 68, 71, 74, 77 and 82 (see Figure 5.2.2).

It was decided to select a period from the boundary conditions provided by Rijkswaterstaat of approximately 12.5 hours duration and cyclic, viz the period from 27 June 1961 17:00 to 28 June 1961 07:30, which was about an average tide. It is again recommended to investigate the impact of a change in the hydrodynamic boundary conditions on the morphological changes in further studies.

The morphological boundary conditions in the form of concentrations are prescribed at all open boundaries of the model, i.e. in the Branches 61, 68, 71, 74, 77 and 82.

5.3 Calibration and validation data

One source of calibration and validation data was available, i.e. the cross-sectional area information in Biegel (1991).

In consultation with Rijkswaterstaat, it was decided to do the calibration using the data of relative cross-sectional areas in the Zoutkamperlaag between 1969 and 1986. The locations of all available cross-sections can be found in Figure 5.3.1 (from: Biegel, 1991). The selected locations for comparison with the model are presented in Figure 5.3.2.

5.4 Calibration and validation

set-up and rough calibration

Similar to the Westerschelde model, the calibration has started with some runs to identify any first problems. During this period, the channels with vertical walls are marked.

The calibration runs directly made clear that some channels in the Pinkegat and the Smeriggat in the model fill up more rapidly than those in Zoutkamperlaag. Such a feature is also found during the two-dimensional model studies such as performed in the framework of Kustgenese (Wang, 1993). It was then also concluded that the time scales of the Pinkegat and the Zoutkamperlaag are different.

In view of the absence of data on the morphological development of the Pinkegat available and the expected small impact of that part of the model on the eastern part, it was decided to cut off the Pinkegat system from the model, west from the Branches 34, 35, 67, 81, 73, 72 and 71 by removal of the relevant branches from the model geometry. The first 8 simulations such as described in Table 5.4.1 were performed with this geometry. After development of procedures to handle channels that fill up, final simulations have been performed which included the Pinkegat and Smeriggat again.

After the initial runs, a rough idea of the ranges for the calibration parameters was formed by changing the relevant parameters considerably. The following parameters have been used as calibration parameters:

- dispersion coefficient for the channel transport, and
- equilibrium concentration.

Based on information provided by Rijkswaterstaat, the fall velocity in the Friesche Zeegat on average is 1 cm/s, which is the value used in the detailed calibration runs.

detailed calibration

The above activities during the rough calibration phase directly resulted in a reasonably good model behaviour. The exact values of the parameters are determined by performing a number of detailed calibration runs, see Table 5.4.1 below.

Run	incl. Pinkegat	c_E [-]	$D_{l/h}$ [m^2/s]	D_c [m^2/s]	Power of equilibrium relation	res. curr. parameter [-]
1	no	0.00001	1	100	4	0.
2	no	**0.00003**	1	100	4	0.
3	no	**0.00005**	1	100	4	0.5
4	no	0.00003	1	100	4	**0.5**
5	no	0.00005	1	100	**2**	0.
6	no	**0.00004**	1	100	3	0.
7	no	0.00004	**10**	100	3	0.
8	no	0.00004	10	**25**	3	0.
9	**yes**	0.0001	1	100	3	0.
10	yes	0.0001	1	**500**	3	0.
11	yes	0.0001	1	**s-v**	3	0.

Table 5.4.1 Overview of calibration runs of the Friesche Zeegat model (not complete). Fat numbers denote the calibration parameter for that run, s-v means: space-varying.

The best results were obtained in Runs 9 and 11, which are worked out in more detail below. It should be noted that most runs showed a good agreement with observations.

Figures 5.4.1 - 5.4.4 present the time series of the various relative cross-sectional areas of 8 cross-sections in the model in correspondence with the observed relative cross-sectional areas below MSL for Run 9 over the period from 1969 to 1988 (20 years). Figures 5.4.5 - 5.4.8 show the similar time series of Run 11. Small jumps in the graphs indicate that a branch has filled up which was part of the cross-section shown and that that branch was deleted from the model.

The agreement between the model results and the observed quantities is very good for both runs, especially in the inner part of the basin. The agreement between the model results and the observations decreases going in the direction of the sea boundary. This can be seen from the results presented in the lower graphs of Figures 5.4.4. and 5.4.8, showing the results for Branch 81.
Most likely, the rapid shallowing of Branch 80 (see Figures 5.4.11 and 5.4.12), which is located directly north of Branch 81, leads to a transport of sediment from Branch 81 (and Branch 67) to Branch 80. As a result, there is not enough sediment (yet) to fill up Branch 81 as well. It is not clear how to solve this problem in the model. In view of the fact that the equilibrium cross-sectional area of Branch 80 decreases during the simulation, this feature may very well be caused by the nodal point relation problem, such as described in Section 3.5.

Note: An (erroneous) run has been performed with a concentration boundary located at the seaward end of Branch 80, whereas the open boundary for the hydrodynamic computation was still located more outward of the system. The results of that run showed that not only the inner part was correct, but also the development of Branch 81 was in a better agreement with the measurement data. This supports the above theory of a deficit of sediment in Branch 81 for a proper simulation of the development.

Run 9 and 11 differ in respect to space-varying dispersion. Space-varying dispersion was introduced in an attempt to improve the results in the Branches 67, 80 and 81. In view of the fact that the development of Branch 81 was much too slow, the value for the dispersion coefficient in the branches around Branch 81 was chosen 250 m^2/s, instead of 100 m^2/s, which was used for the other parts of the model. Figures 5.4.4 and 5.4.8 make clear that there is not much improvement, although more channels filled up. The silted channels are summarized in Table 5.4.2 for the Runs 9 and 11. In the table the year of total filling up of branches for each of these runs is listed.

Run	Branch number (location see Figure 5.2.2)										
	26	29	32	42	58	59	60	61	62	63	65
9		1981	1977	1969						1984	1970
11	1980	1974	1977	1969	1984	1983	1984	1984	1984	1975	1970

Table 5.4.2 Year of total filling up of branches for the Runs 9 and 11

Table 5.4.2 shows that, although the time series of Runs 9 and 11 (see Figures 5.4.1 - 5.4.8) are very much alike, the filling up of channels is subject to different time scales as a result of different values for the dispersion coefficient.

In order to give an indication of the development of the cross-sectional profile along the basin, such profiles are plotted in Figures 5.4.9 - 5.4.12.

Figures 5.4.9 and 5.4.10 present the profiles in the years 1969 and 1988 for the entrance of the Zoutkamperlaag and for approximately the centre area of the Zoutkamperlaag, respectively. These figures show that at the entrance of the basin, not only the main channel of the Zoutkamperlaag is shallowing, but also the middle channel of the Gat van Schiermonnikoog is. More to the head of the basin, the channel of the Gat van Schiermonnikoog, which is located parallel to the Zoutkamperlaag, is deepening, whereas the Zoutkamperlaag is shallowing.

Table 5.4.2 makes clear that channels are silting up in the west of the Pinkegat. In order to have some idea on the difference of the computed development of the channels in the ebb tidal delta between Run 9 and 11, a cross-section was defined from east to west across the tidal inlet (Branches 87, 85, 80, 73, 70, 63, 62). Figures 5.4.11 and 5.4.12 present the bed profile along this cross-section in the years 1969 and 1988 for Run 9 and Run 11, respectively. From these figures it appears that the differences in the results of these two runs with respect to the cross-section shown, is not so large as expected. It is concluded that the tendency of the development (deposition, erosion) is the same, but the time scale is different. It is remarkable that the main Channel 80 is silting up, but its function is taken over by Branch 73, located west of Branch 80, which is deepening.

5.5 Conclusions

A morphological model of the Friesche Zeegat has been set up. In view of the different time scales of the Pinkegat and Smeriggat compared to the Zoutkamperlaag and of the relative unimportance of those areas for the simulation, simulations have been performed both with the whole Friesche Zeegat system and with the Pinkegat system removed from the original model.

In view of the small amount of data, the calibration and validation of the model is combined to one period of 18 years (1969-1986). The calibration has been performed on cross-sectional areas during this period.

The results of the model are in very good agreement with observations.

Based on the above, the predictive ability of the model is expected to be good. It can therefore after some adaption very well be used to determine the future morphological development of the Zoutkamperlaag.

6 Conclusions and recommendations

6.1 Conclusions

the software system

A software system to simulate the long-term morphological development of estuaries (ESTMORF) is developed according to the functional requirements laid down in Karssen and Wang (1993), implemented and tested.

Comprehensive tests are performed with the software, in the form of debugging, prototype testing and real model testing.
The tests show that:

- the software is correct from a programming point of view.
- the numerical solution method is correct and correctly implemented.
- the results of morphological computations with the software for prototype models are exactly in line with results of theoretical analyses,
- the present nodal point relations may lead to instabilities in the behaviour of the channels behind a bifurcation,
- the impacts of land subsidence and sea level rise are correctly implemented.

A sensitivity analysis for a prototype tidal basin is performed in order to get a feeling for the values of the parameters and their impact on the results.

A set of post-processing programs is developed which makes it possible to write to file relevant quantities, such as:

- time series of the cross-sectional area below MSL,
- volume changes for groups of branches over a period,
- time series of cross-sectional profiles, and
- the total volume of human interference.

Restart software programs are written to facilitate the removal of branches which have filled up and adapt the other input files.

ESTMORF has proven to be a robust and flexible software system that is very suitable for research purposes in complex estuarine systems, such as the Westerschelde, but can also as yet be used for consultancy with respect to more simple estuarine or tidal basin systems, such as the Friesche Zeegat.

the Westerschelde model

A morphological model is built of the Westerschelde, which is calibrated as good as possible using the available data and within the available time.

The filling up of a number of channels in the Westerschelde is simulated properly. For example, the development of the Platen van Valkenisse is well predicted by the model.

The computed relative cross-sectional changes between 1977/78 and 1992 are in reasonable agreement with observations, but the results are certainly not yet perfect.

The agreement of the computed and observed volumetric changes is reasonable to good, and varies somewhat over the Westerschelde area. Near the mouth of the Westerschelde up to Hansweert, the model results compare very well with the measured volumes. In the area east of Hansweert, the comparison is slightly worse, although the tendency is correct. A shift of the dumping and dredging volumes from the Land van Saeftinghe to the area near Bath in combination has led to a considerable improvement of the model results in that area (Karssen, 1995).

The form of the empirical relations for the tidal flats in the Westerschelde model are copied from those for the Wadden Sea. This may lead to an incorrect model behaviour.

The impact of the hydrodynamic boundary conditions on the results is not clear. A 12.5 hours cyclic period has been selected from data provided, but in how far other boundary conditions would have affected the results is not studied.

The Westerschelde model is not (yet) suitable for predictive purposes. The present model has to be considered as a first version or a working prototype. As more field data comes available and the behaviour of the development of estuaries is better understood, the model and the software will be improved in order to make the model suitable for more general predictive purposes as well.

the Friesche Zeegat model

A morphological model of the Friesche Zeegat has been set up and calibrated for the basin east of Engelsmansplaat.

The results of the model are in very good agreement with observations. The morphological development of Zoutkamperlaag after the closure of the Lauwerszee in 1969 is simulated properly.

The predictive ability of the model is expected to be good. It can therefore very well be used to determine the future morphological development of the Zoutkamperlaag.

Due to the absence of field data on the heights of the tidal flats, the calibration of the Friesche Zeegat model focused on the development of the channels. Therefore, it is unclear how the model represents the development the tidal flats (see also the recommendations in Section 6.2).

6.2 Recommendations

the software system

The hydrodynamic model IMPLIC is suitable for the present applications, but the modelling system SOBEK will become the standard for one-dimensional modelling at Rijkswaterstaat and DELFT HYDRAULICS in the near future. It is recommended to develop a link between SOBEK and ESTMORF as soon as possible. In view of the flexibility of ESTMORF, this will not be a difficult task.

New nodal point relations should be implemented in ESTMORF after the definition of these relations as part of the EENDMORF study.

Human interference by dredging and dumping now only takes place in the channel. It is recommended to work out a procedure to distribute sediment over the profile sections (channel, low/high flats), including the corresponding relations for profile change.

A post-processing system should be set up, based on the programs such as developed in the present study, including the coupling with a graphical software package.

Experience should be built up with the software by setting up models of other estuaries and tidal basins, and the further calibration of the Westerschelde model.

The calibration parameters of ESTMORF, such as the equilibrium concentration, diffusion coefficients and fall velocity, have the same dimension and name as the well-known parameters in the standard advection-diffusion equation for suspended sediment transport. However, the values for the parameters are not necessarily of the same (order of) magnitude as their standard appearance. It is recommended to study the physical background of these parameters and work out a method to determine these parameters from physical quantities. A more fundamental study, such as performed in the framework of EENDMORF, would be a proper way to achieve this.

the Westerschelde model

The Westerschelde model can be improved by extensive calibration, using suitable calibration data. It is recommended to do this by setting up an additional calibration phase, in which the available data is analyzed on its reliability and practical use for the model. It is expected that calibration on volume changes (or cross-sectional areas) per branch of the model would be a proper and suitable method.

Further, the suitability of the present hydrodynamic model for morphological computations should be studied. The present hydrodynamic model has been set up with the purpose to simulate the hydrodynamics (especially water levels) properly, but not for morphological purposes. With respect to this, special attention should be paid to the schematisation of the geometry (see also Allersma (1993)).

References

Allersma, E., 1993: Geulen in estuaria, 1-D modellering van evenwijdige geulen. Report H1828/H1970. DELFT HYDRAULICS, Delft, December 1993. (In Dutch; in preparation)

Biegel, E.J., 1991: Equilibrium relations in the ebb tidal delta, inlet and backbarrier area of the Frisian Inlet system. Kustgenese/Coastal Genesis. Report GEOPRO 1991.028/GWAO-91.016. Faculty of Geographical Sciences, University of Utrecht, Utrecht, November 1991.

Dongeren, A. van, 1992: A model of the morphological behaviour and stability of channels and flats in tidal basins. M. Sc. Thesis, Report H824.55. Delft University of Technology/DELFT HYDRAULICS, Delft, March 1992

Eysink, W.D. 1992: Impact of sea level rise on the morphology of the Wadden Sea in the scope of its ecological function, Volume I. Report H1300. DELFT HYDRAULICS, Delft, December 1992.

Jeuken, M.C.J.L., 1993: Morfologische veranderingen van de platen en geulen in de Westerschelde gedurende de periode 1965-1990 (in Dutch). Nota NWL-93.13. Rijkswaterstaat Direktie Zeeland. March 1993.

Karssen, B., 1994: A dynamic/empirical model for the long-term morphological development of estuaries, Part II: Development of the model, Phase I. Report Z715. DELFT HYDRAULICS, Delft, January 1994.

Karssen, B., 1995: Evaluation of ESTMORF; Mass balance and additional simulation. Report Z891. DELFT HYDRAULICS, Delft, March 1995.

Karssen, B. and Z.B. Wang, 1991a: Note on preliminary study of ESTMORF. DELFT HYDRAULICS, Delft.

Karssen, B. and Z.B. Wang, 1991b: Morphological modelling in estuaries and tidal inlets, Part I: A literature survey. Report Z473. DELFT HYDRAULICS, Delft, December 1991.

Karssen, B. and Z.B. Wang, 1992: A dynamic/empirical model for the long-term morphological development of estuaries. Note Z473.20. DELFT HYDRAULICS, Delft, October 1992.

Karssen, B. and Z.B. Wang, 1993: A dynamic/empirical model for the long-term morphological development of estuaries, Part I: Physical relations. Report Z622. DELFT HYDRAULICS, Delft, April 1993.

Svasek, 1994: Verklarend onderzoek Drempels Westerschelde. Projekt 940. January 1994.

Van den Berg, J.H., D. Schouten and C.J. van Westenbrugge, 1991: Zandbalans Westerschelde 1965-'70-'75-'80-'85. Nota NWL-91.36. Rijkswaterstaat, Direktie Zeeland. April 1991.

Wang, Z.B., 1993: Morphological Modelling for a Tidal Inlet in the Wadden Sea; Het Friesche Zeegat. Progress Report Part III, Report H840. DELFT HYDRAULICS, Delft, January 1993.

Wang, Z.B., R.J. Fokkink and B. Karssen, 1993: Theoretical analysis on nodal point relations in one-dimensional morphodynamic models, Report Z473-II, DELFT HYDRAULICS, Delft.

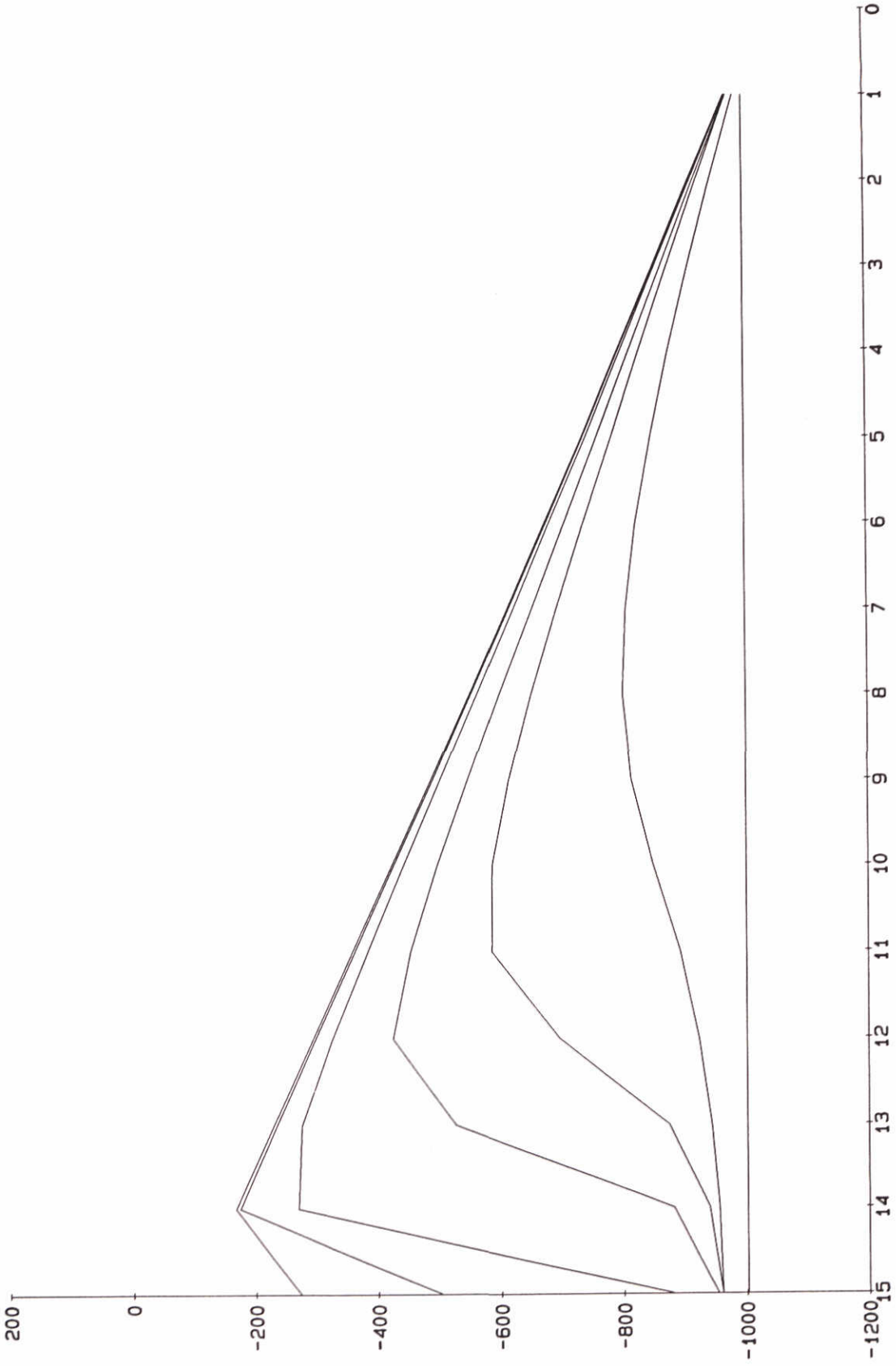

No flats
Dc= 10. Ws= 0.001 Conc = 0.001 PowerA= 4.

Run : 000

ESTMORF

DELFT HYDRAULICS

Proj: Z-715

Fig. 3.2.1

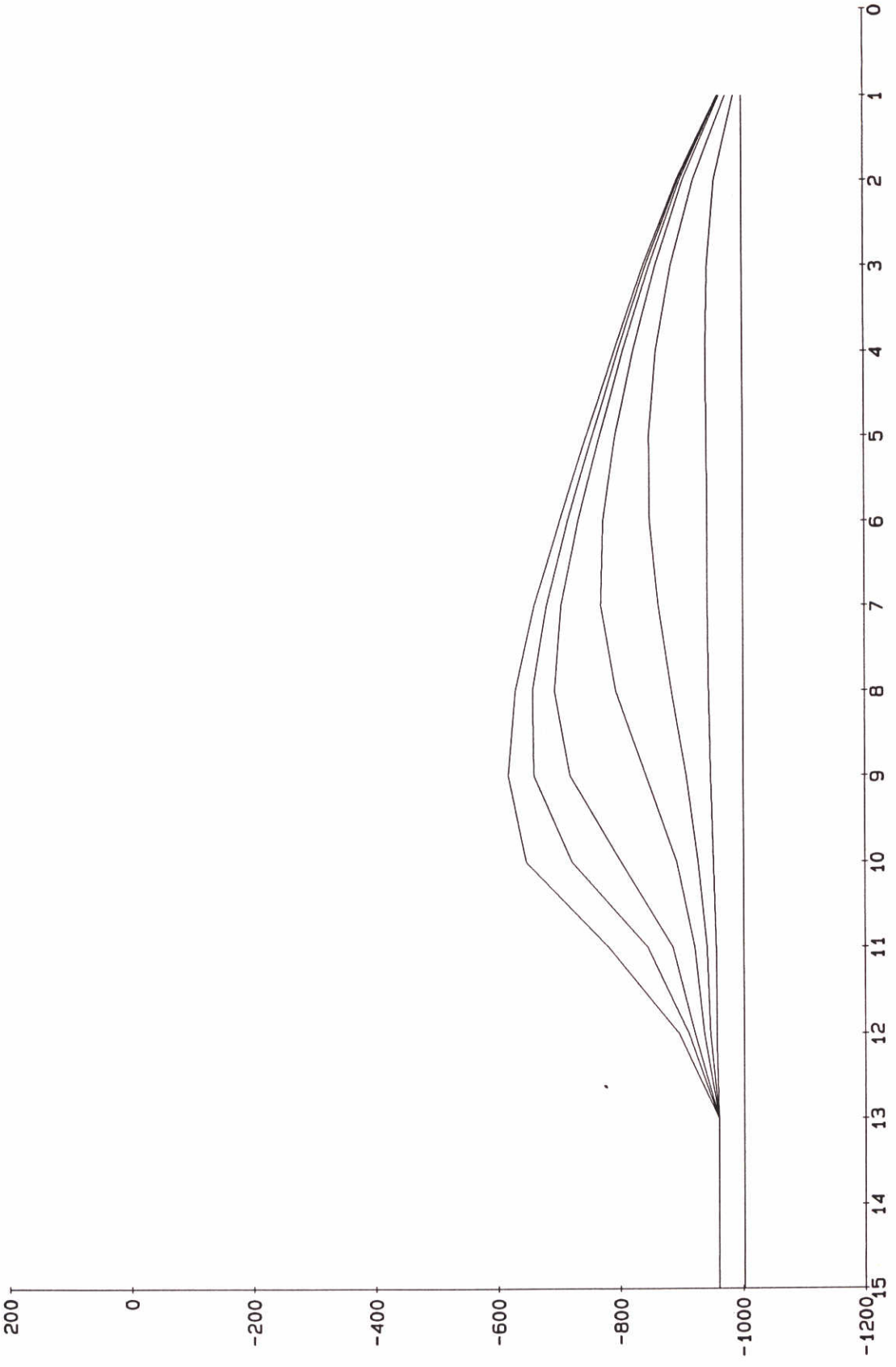

No flats
Dc= 1. Ws= 0.001 Conc= 0.001 PowerA= 4.

Run : 021

ESTMORF

DELFT HYDRAULICS

Proj: Z-715

Fig. 3.2.4

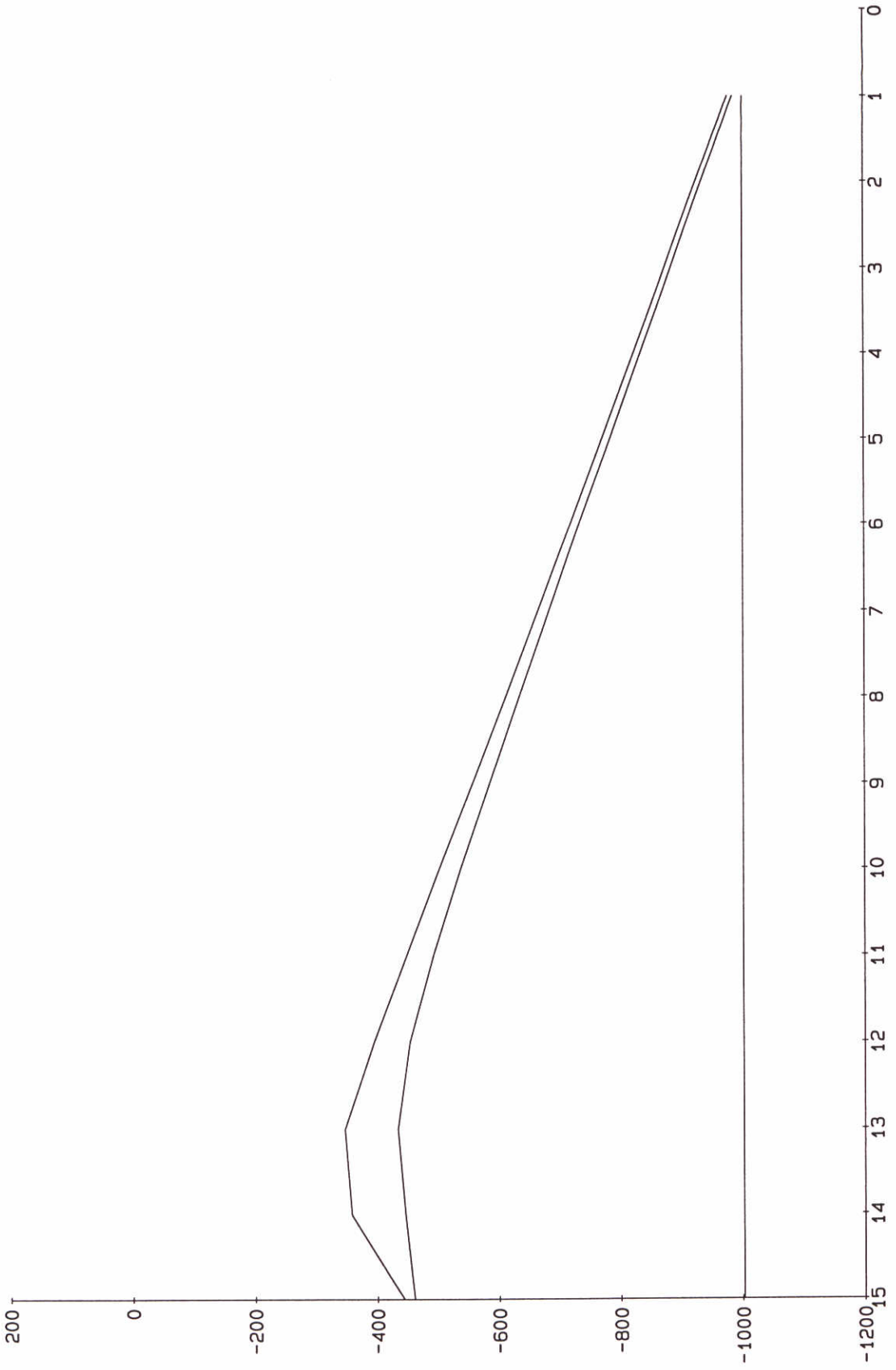

No flats
Zelfde als 021 maar dan Dc=20. i.p.v. 1.0

Run : 022

ESTMORF

DELFT HYDRAULICS

Proj: Z-715

Fig. 3.2.5

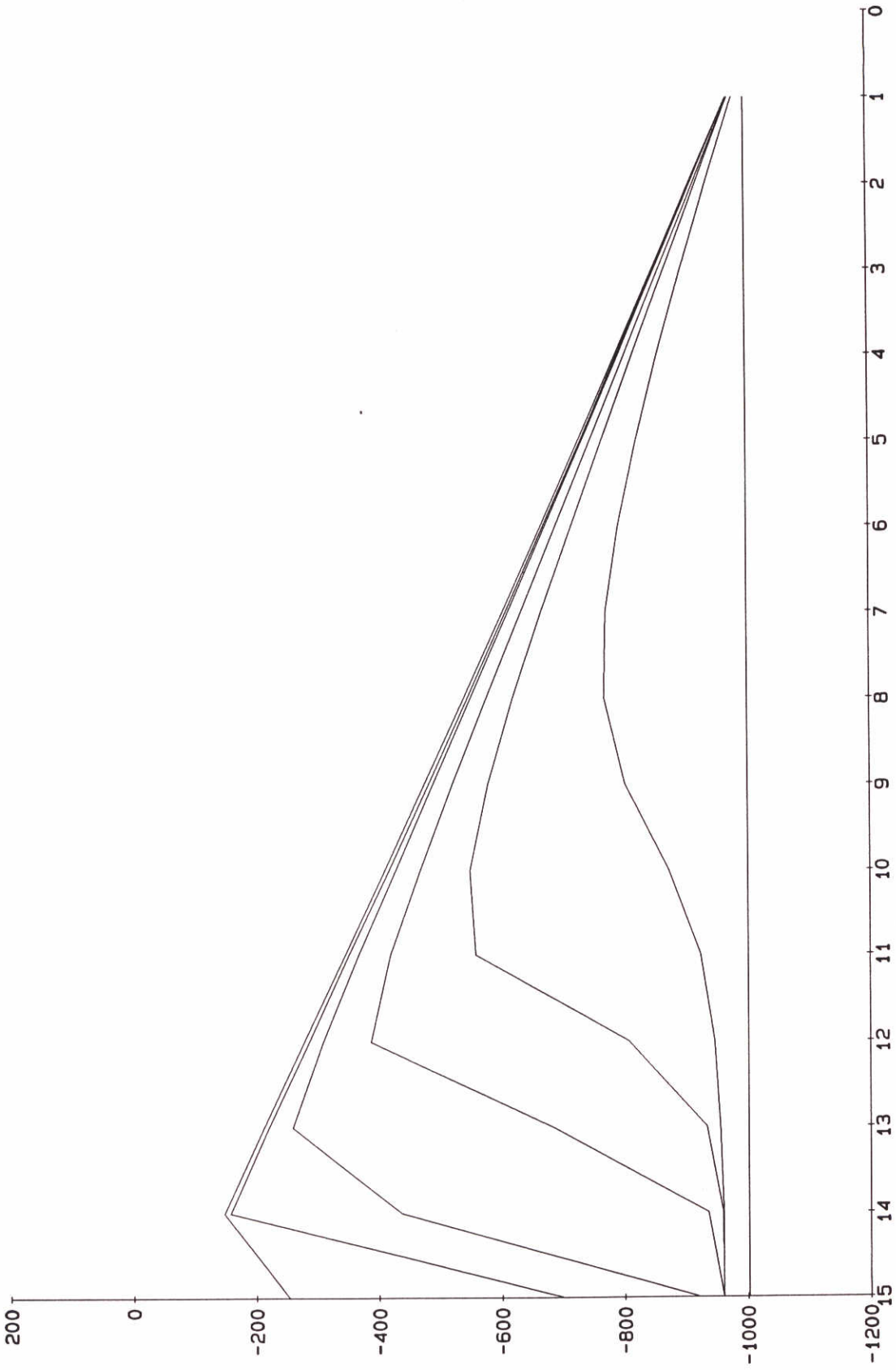

No flats
Dc= 10. Ws= 0.001 Conc= 0.001 PowerA= 5.

Run : 042

ESTMORF

DELFT HYDRAULICS

Proj: Z-715

Fig. 3.2.9

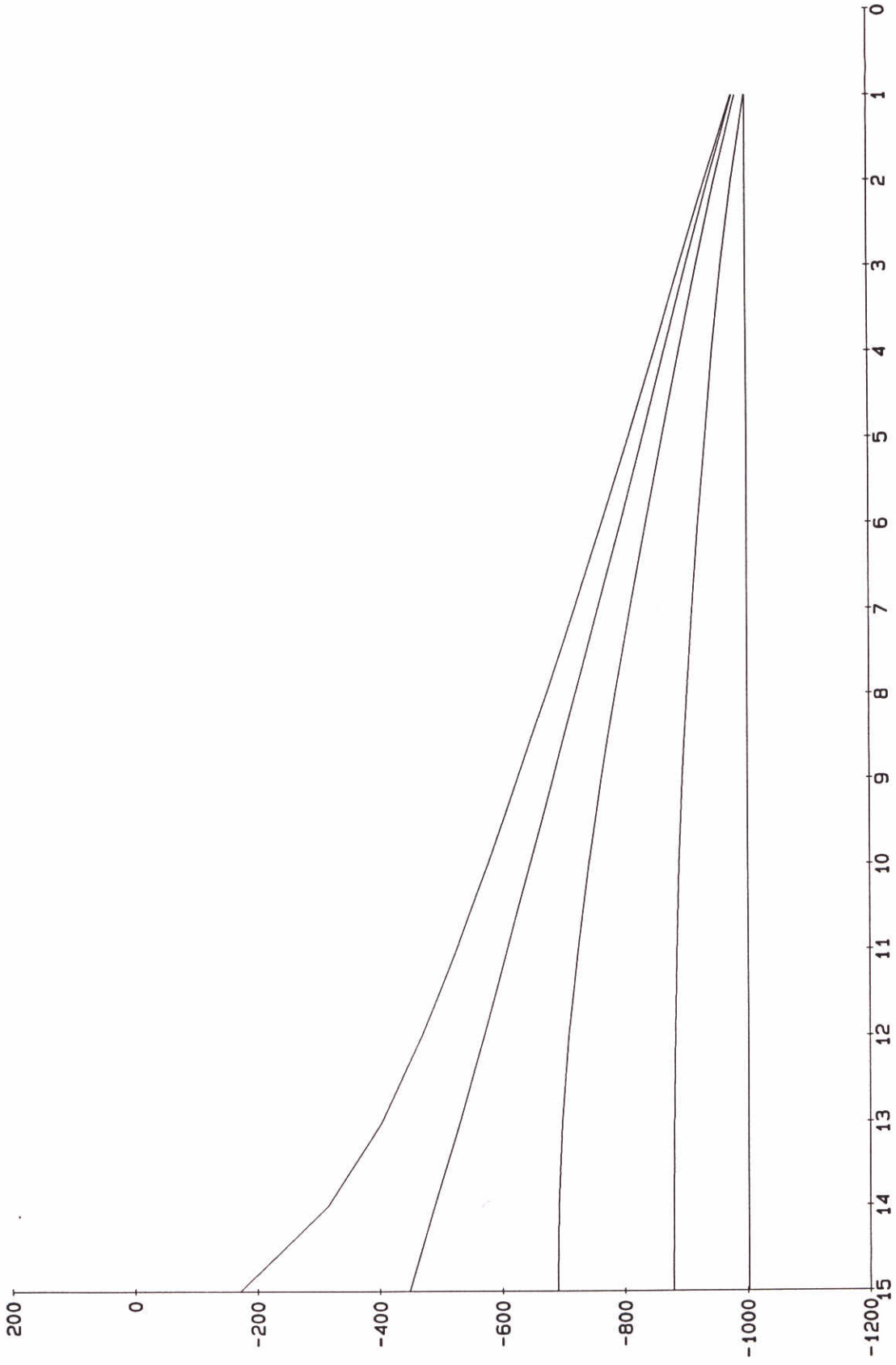

No flats Zelfde als 041 maar dan PowerA= 2. i.p.v. 3.	Run : 045	
	ESTMORF	
DELFT HYDRAULICS	Proj: Z-715	Fig. 3.2.10

t = 0

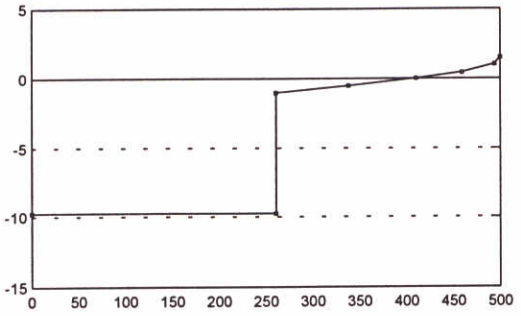

t = 4

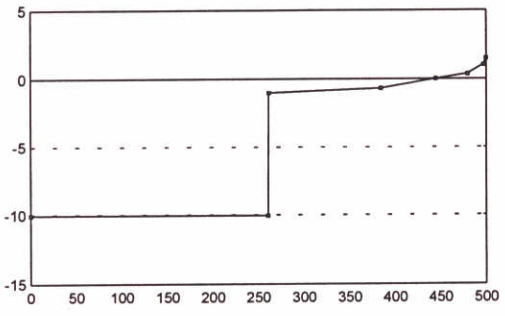

t = 8

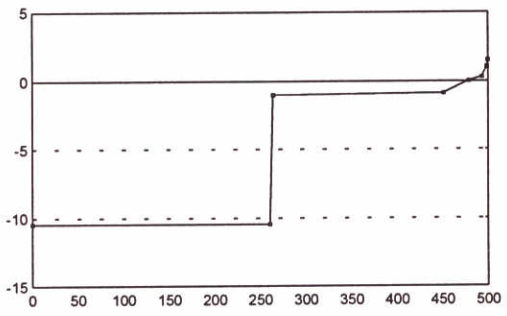

t = 12

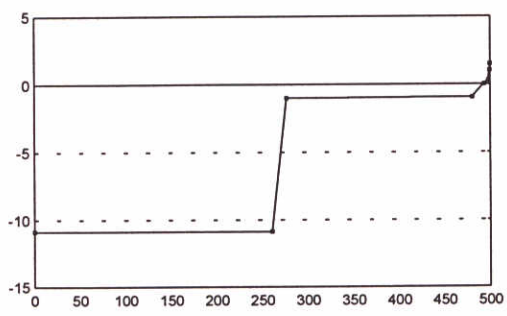

Profile changes Land subsidence test		Nov 1994
	ESTMORF	
DELFT HYDRAULICS	Z-715	Fig.3.4.1

Westerschelde

Implic vakindeling 1968/69
Bodem 1971/72

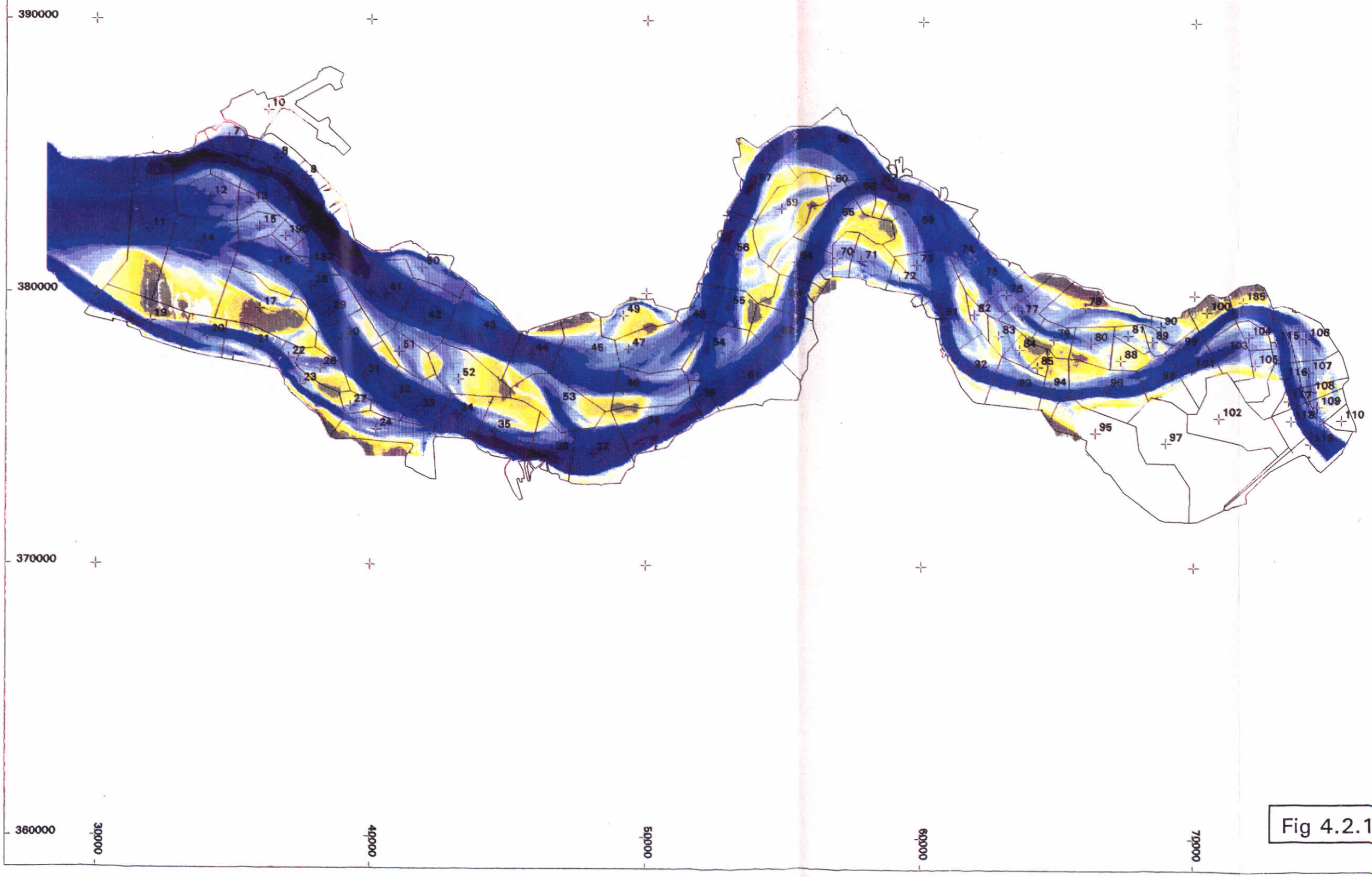

Legenda
meters

- 3.9 t/m 3
- 3 t/m 2
- 2 t/m 1
- 1 t/m 0.5
- 0.5 t/m 0
- 0 t/m -0.5
- -0.5 t/m -1
- -1 t/m -2
- -2 t/m -3
- -3 t/m -5
- -5 t/m -7.5
- -7.5 t/m -10
- -10 t/m -15
- -15 t/m -20
- -20 t/m -30
- -30 t/m -40
- -40 t/m -61.7

Schaal: 1:150.000

Fig 4.2.1

Oostwest
Rijksinstituut voor Kust en Zee
Rijkswaterstaat

Arc-Info applicatie PlotGIS
Drs. L.A. Uit den Bogaard

INDIEN GEEN AFWIJKENDE WAARDE
BIJ DE SECTIES IS VERMELD GELDT
VOOR ZOWEL EB ALS VLOED
K = 40

RIVIER Nr 24
SECTIECOMBINATIE 10106

GET	GEZ	GEC	AKK	GETIJBEREKENING WESTERSCHELDE, SCHELDE EN ZIJRIVIEREN NETWERK MET NUMMERING SECTIES Nr S17V MET BIJBEHORENDE K-WAARDEN	L75001 T016	
A.S.B.				RIJKSWATERSTAAT - DIRECTIE WATERHUISHOUDING EN WATERBEWEGING STUDIEDIENST VLISSINGEN	B 2	77.692

VLISSINGEN
BRESKENS
HOOFDPLAAT
BORSSELE
HOEDEKENSKERKE
BAARLAND
OSSENISSE
ELLEWOUTSDIJK
TERNEUZEN
HANSWEERT
WAARDE
PERKPOLDER
BAALHOEK
BATH
HEDWIGEPOLDER
LEIDAM BALLASTPLAAT
PROSPERPOLDER
LIEFKENSHOEK
BOUDEWIJNSLUIS
ST MARIE
EMBLEM
ANTWERPEN
HEMIKSEM
SCHELDE
LIER
KESSEL
DUFFELSLUIS
DUFFEL
NETE
SCHELLE
HINGENE
BOOM
RUPEL
WALEM
DÜLE
MECHELEN
ZENNE
ZEMST
TEMSE
TIELRODE
DURME
LOKEREN
ZELE
MANTA
WAASMUNSTER
WAASMUNSTER SLUIS
GENTBRUGGE
MELLE
WETTEREN
SCHOONAARDE
UITBERGEN
DENDERMONDE
ST AM. NDS

TOELICHTING:

70
(69)
43 E33 V31 47

SECTIE, MET IN HET MIDDEN HET BIJ DE GETIJBEREKENING VOLGENS DE VOORWAARTS IMPLICIETE DIFFERENTIEMETHODE, OPLOSSINGSMETHODE BEGEMAN, GEBRUIKTE SECTIENUMMER, TUSSEN ( ) HET SECTIENUMMER VOLGENS DE SCHEMATISATIE, AAN DE UITEINDEN DE KNOOPPUNTNUMMERS: AAN DE ONDERZIJDE DE K-WAARDE VOOR VLOED (V30) EN EB (E30) INDIEN DEZE AFWIJKEND ZIJN VAN DE IN HET KADER VERMELDE WAARDE

DE POSITIEVE STROOMRICHTING IN EEN SECTIE LOOPT VAN HET LAGE KNOOPPUNTNUMMER NAAR HET HOGE. BIJ SECTIES, WAAR DE RICHTING NIET OP DEZE WIJZE IS TE BEPALEN OF DIE HIERVAN AFWIJKEN, IS DE POSITIEVE RICHTING AANGEGEVEN DOOR ⟶
DE INGAANDE ZIJDE VOLGENS DE POSITIEVE STROOMRICHTING VAN EEN SECTIE WORDT AANGEDUID MET .1 ACHTER HET SECTIENUMMER B.V. 98.1
DE UITGAANDE ZIJDE MET .2, B.V. 98.2 .
SCHEMATISATIE BOVENSTROOMS VAN KNOOPPUNT BIJ SCHELLE VOLGENS GEGEVENS GETIJBEREKENING S.V. 1953, RAPPORT „STORMVLOEDEN OP DE SCHELDE", DEEL X, VAN WATERBOUWKUNDIG LABORATORIUM BORGERHOUT

PEILSCHAAL (REG.)
PEILSCHAAL (VIS.)
MEETRAAI

Fig 4.2.2

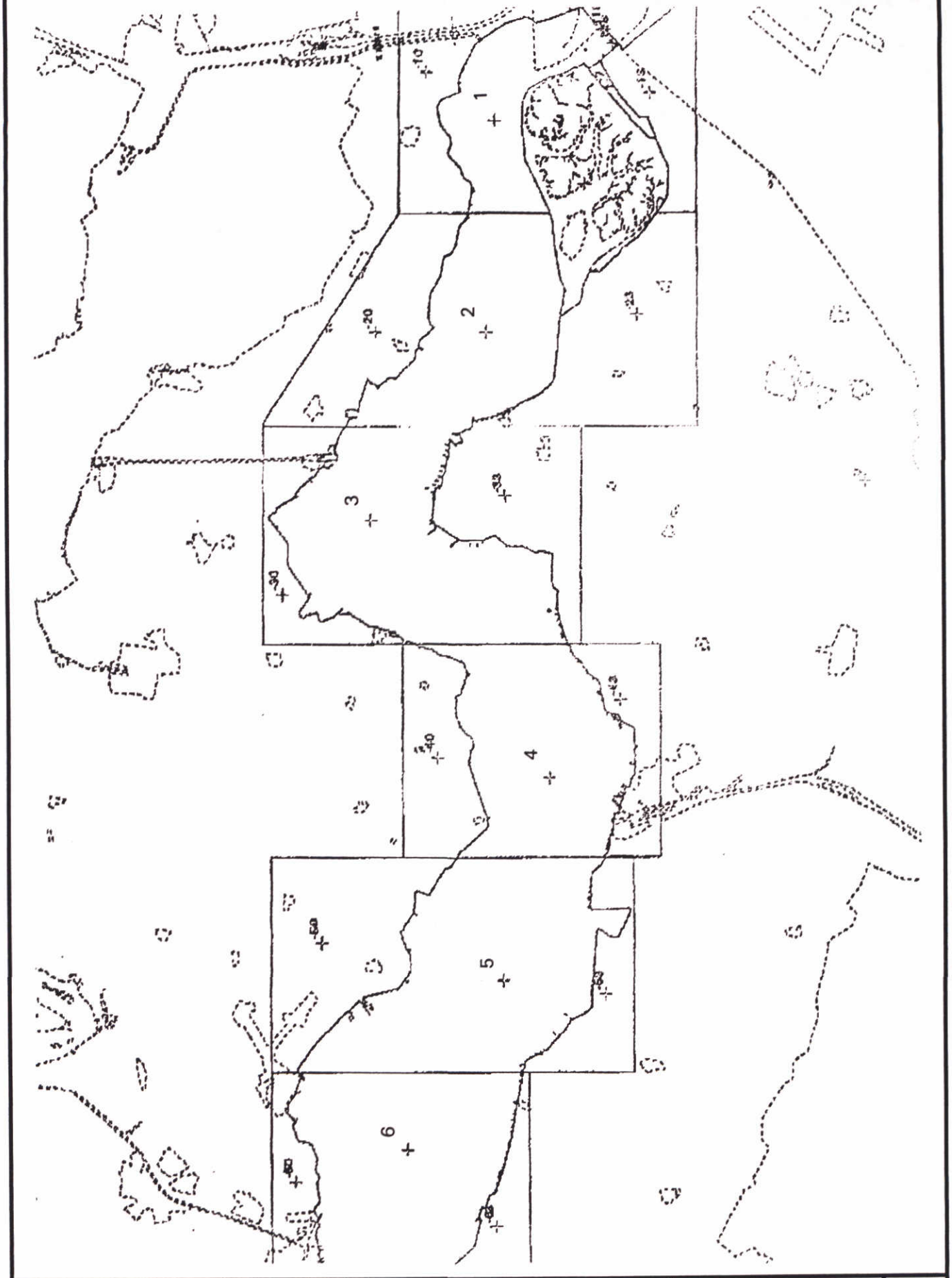

Subdivision of the volume areas.

A4

DELFT HYDRAULICS

Fig 4.3.1

Relative change between 1977/78 and 1992

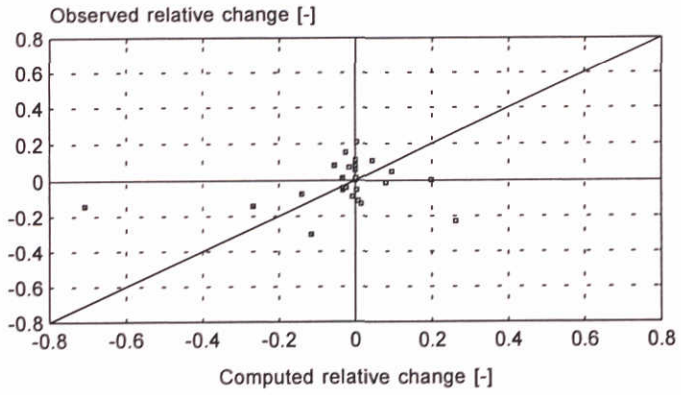

Runid:100/101

Area in 1977/78

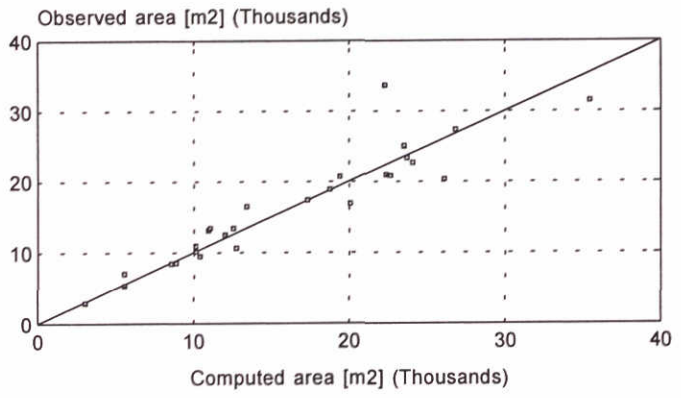

Runid: 100/101

Area in 1992

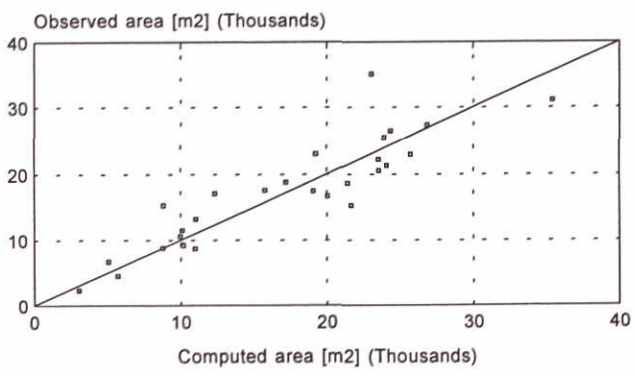

Runid: 100/101

Cross-sectional area results Run 100		Nov 1994
	ESTMORF	
D E L F T H Y D R A U L I C S	Z-715	Fig.4.4.1

Relative change between 1977/78 and 1992

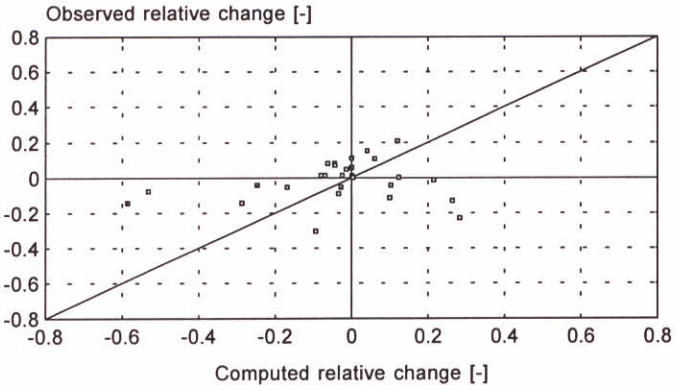

Runid:110/...

Area in 1977/78

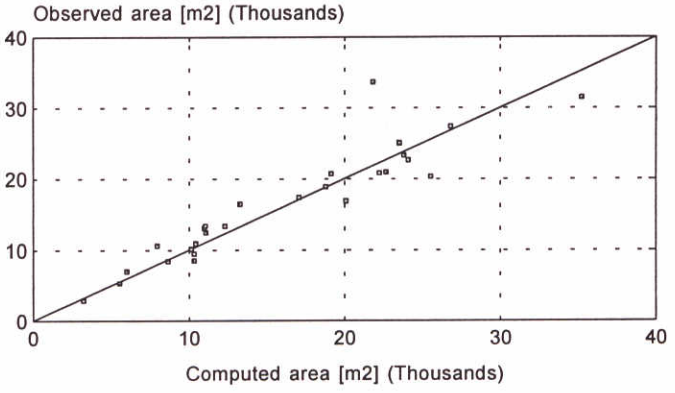

Runid: 110/...

Area in 1992

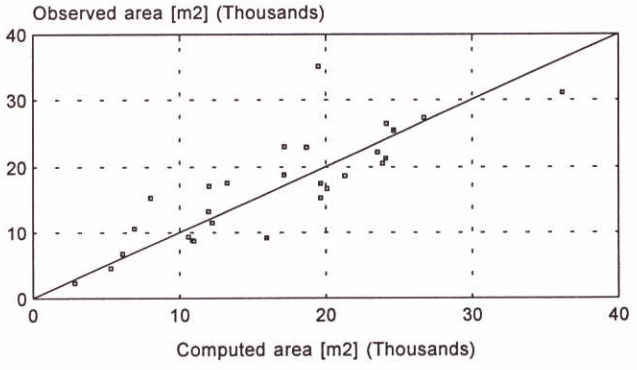

Runid: 110/...

Cross-sectional area results Run 110		Nov 1994
	ESTMORF	
D E L F T H Y D R A U L I C S	Z-715	Fig.4.4.2

Relative change between 1977/78 and 1992

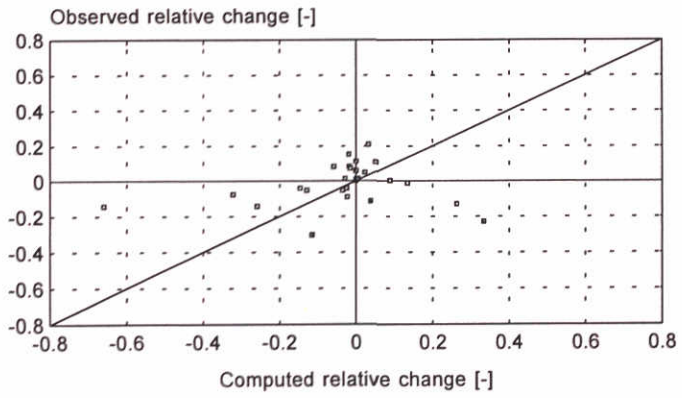

Runid:300/...

Area in 1977/78

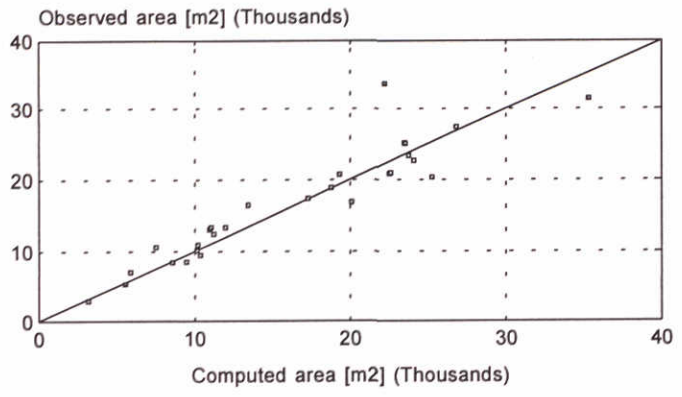

Runid: 300/...

Area in 1992

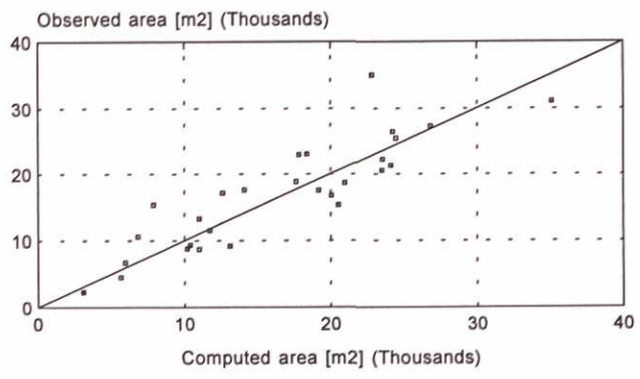

Runid: 300/...

Cross-sectional area results Run 300		Nov 1994
	ESTMORF	
D E L F T H Y D R A U L I C S	Z-715	Fig.4.4.3

Area 1

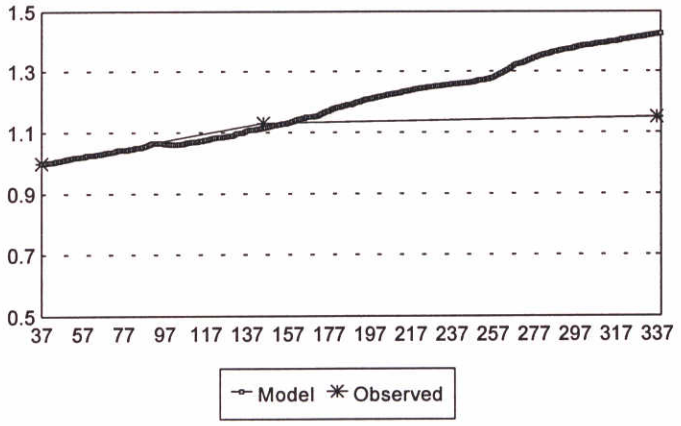

100

Area 2

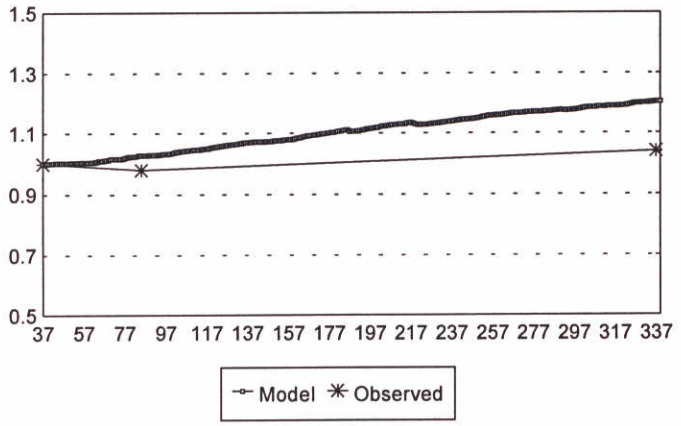

100

Area 3

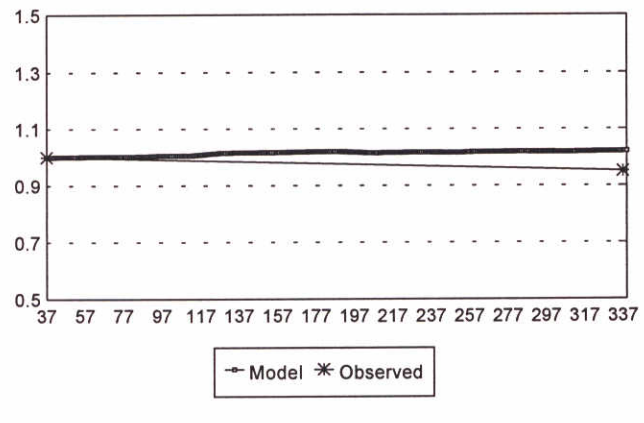

100

Volumetric results 1968 - 1993 Run 100 Areas 1, 2 and 3		Nov 1994
	ESTMORF	
D E L F T H Y D R A U L I C S	Z-715	Fig.4.4.4

Area 4

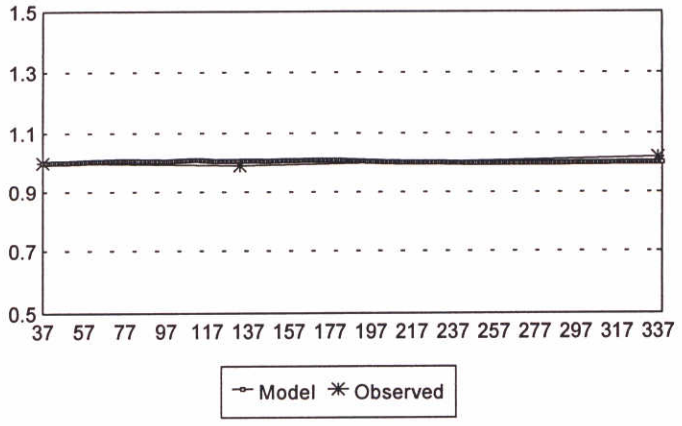

100

Area 5

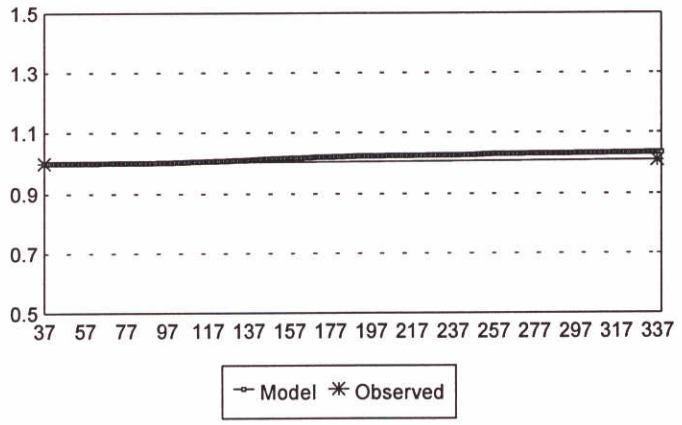

100

Area 6

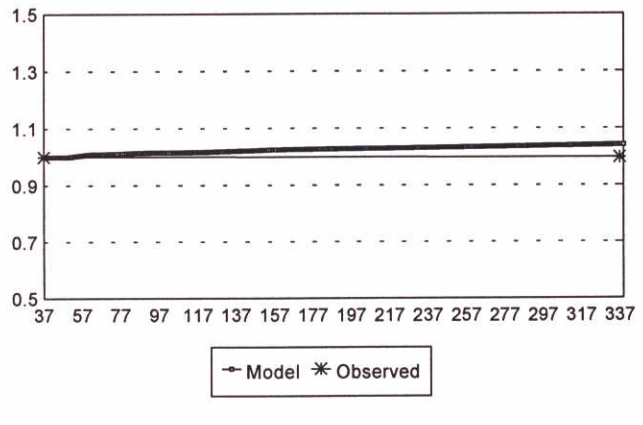

100

Volumetric results 1968 - 1993 Run 100 Areas 4, 5 and 6		Nov 1994
	ESTMORF	
DELFT HYDRAULICS	Z-715	Fig.4.4.5

Area 1

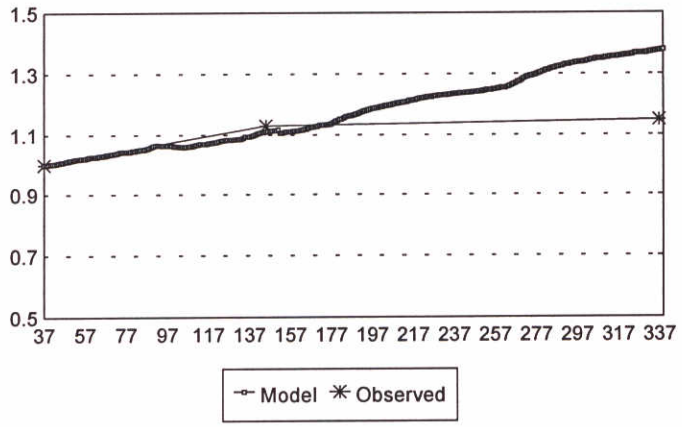

300

Area 2

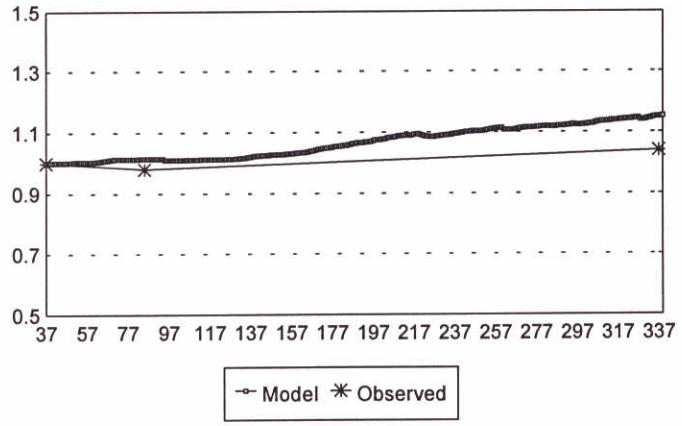

300

Area 3

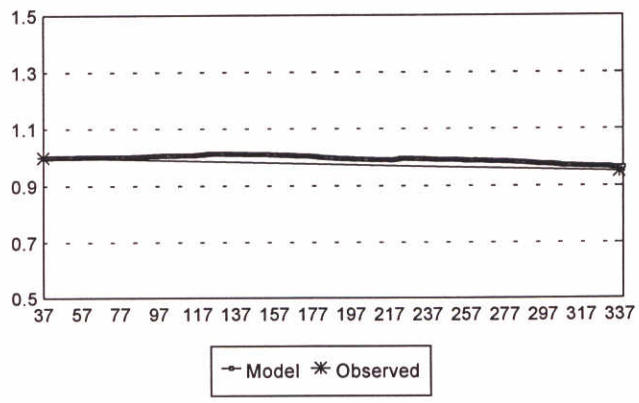

300

Volumetric results 1968 - 1993 Run 300 Areas 1, 2 and 3		Nov 1994
	ESTMORF	
D E L F T H Y D R A U L I C S	Z-715	Fig.4.4.6

Area 4

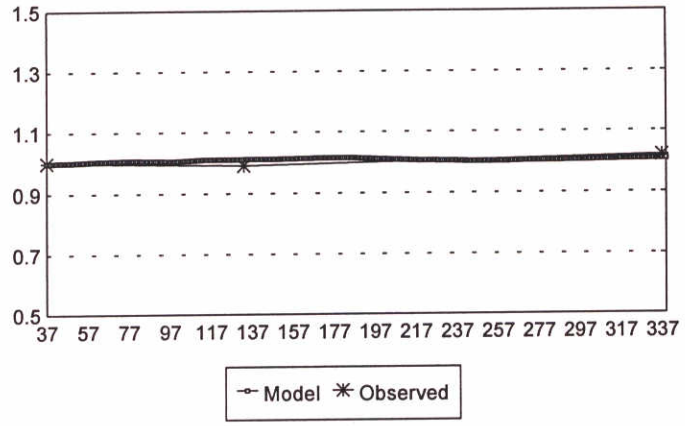

300

Area 5

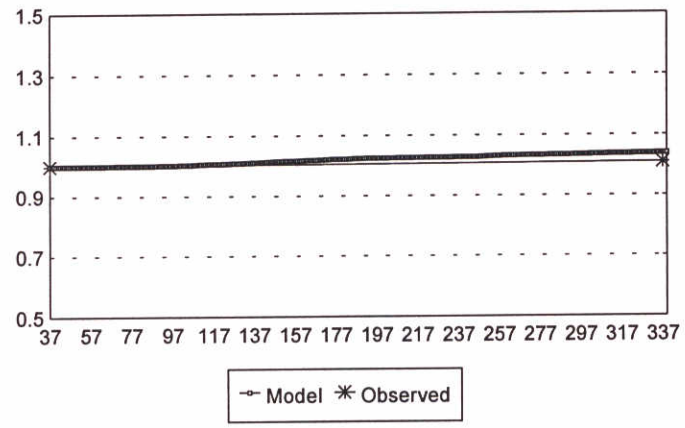

300

Area 6

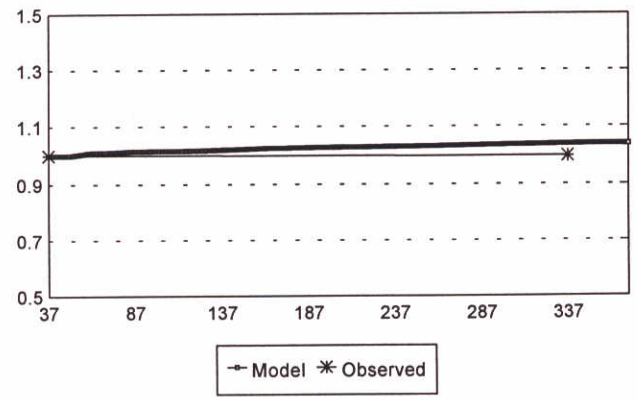

300

Volumetric results 1968 - 1993 Run 300 Areas 4, 5 and 6		Nov 1994
	ESTMORF	
DELFT HYDRAULICS	Z-715	Fig.4.4.7

1968

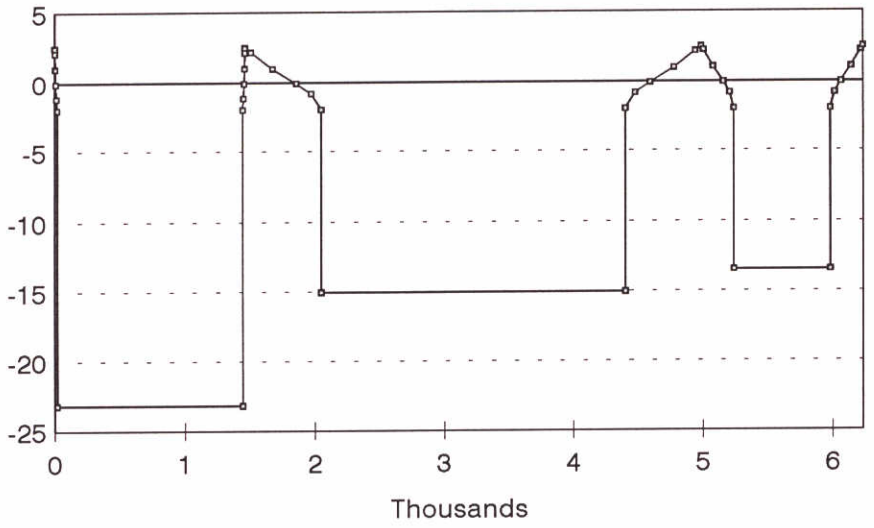

entrance

1993

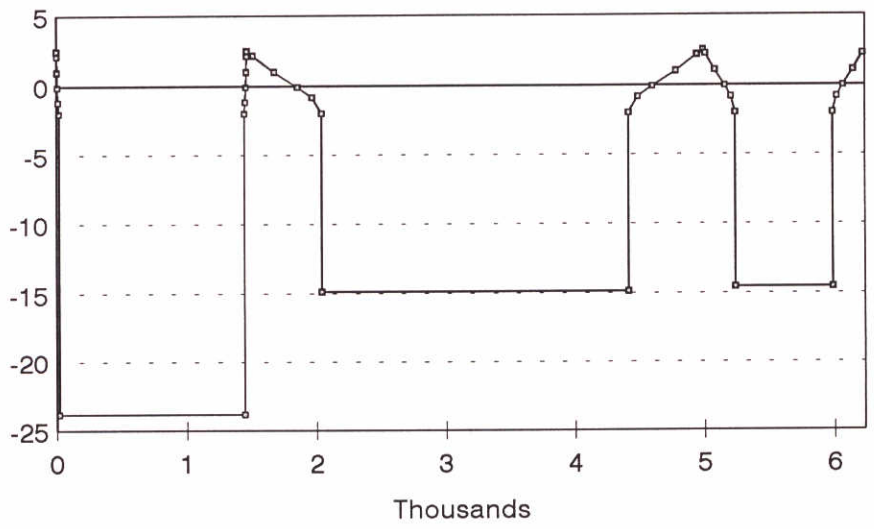

entrance

Computed cross-sectional profile 1968 and 1993 Entrance of the Westerschelde Run 300		Nov 1994
	ESTMORF	
DELFT HYDRAULICS	Z-715	Fig.4.4.8

1968

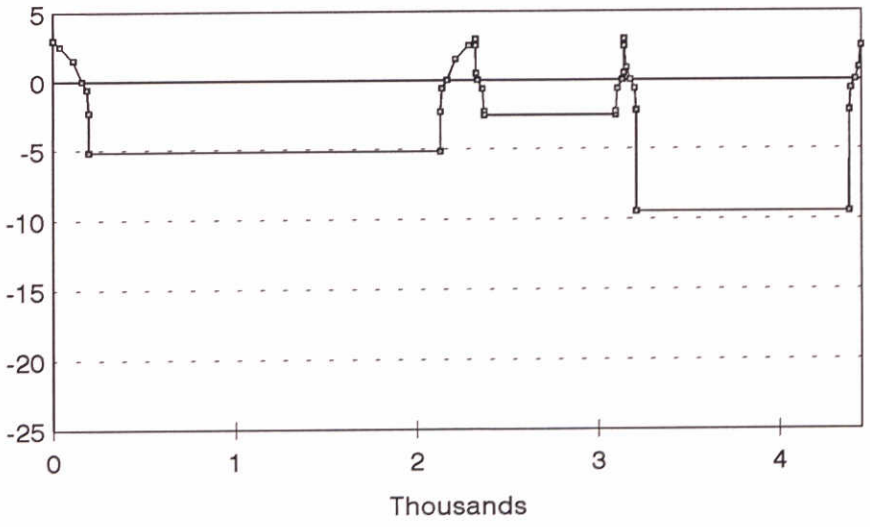

Valkenisse

1993

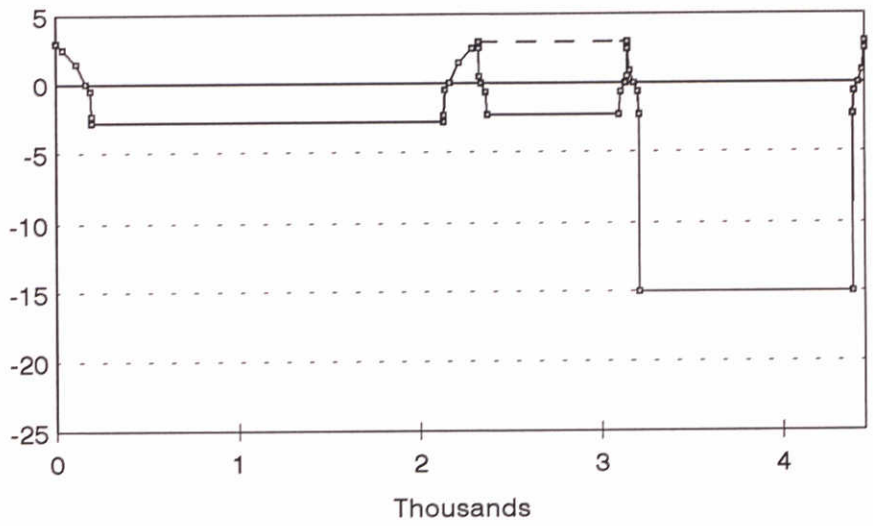

Valkenisse

Computed cross-sectional profile 1968 and 1993 Near Valkenisse Run 300		Nov 1994
	ESTMORF	
D E L F T H Y D R A U L I C S	Z-715	Fig.4.4.9

Area 1

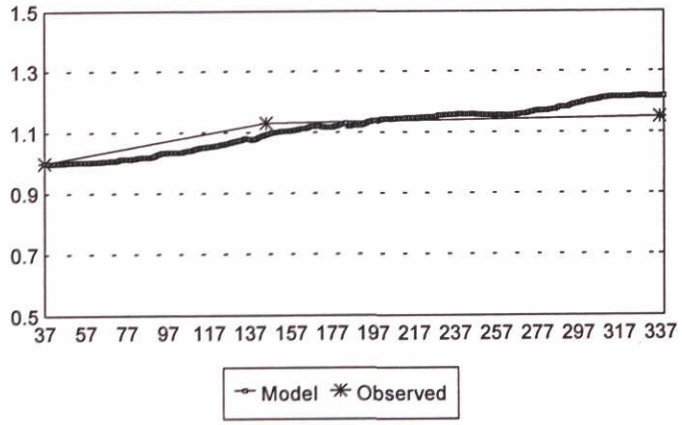

500

Area 2

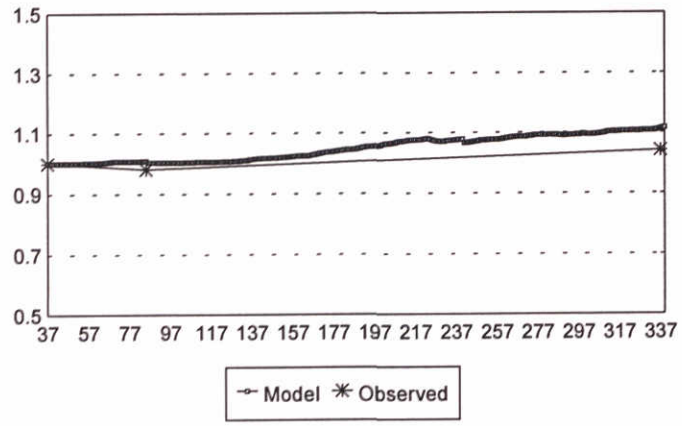

500

Area 3

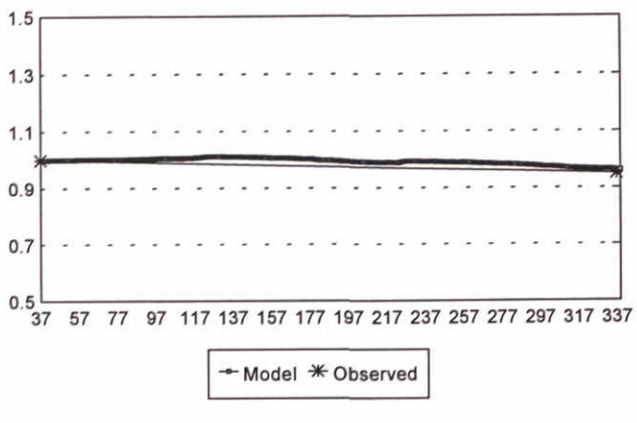

500

Volumetric results 1968 - 1993 Run 500 Areas 1, 2 and 3		Nov 1994
	ESTMORF	
DELFT HYDRAULICS	Z-715	Fig.4.4.10

Area 4

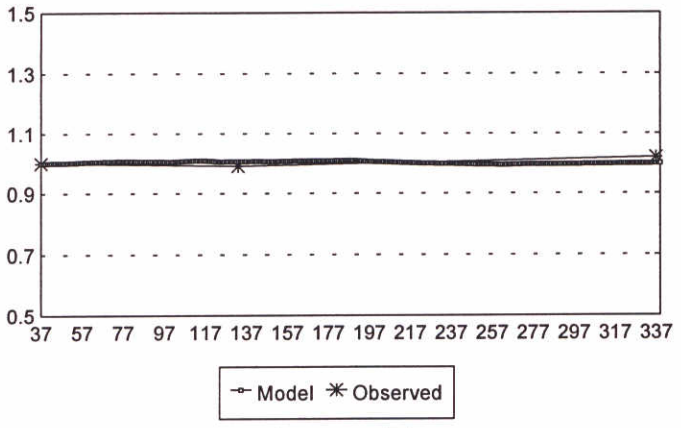

500

Area 5

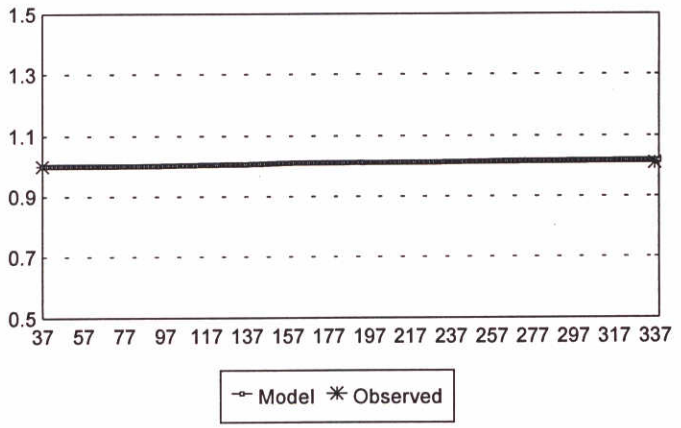

500

Area 6

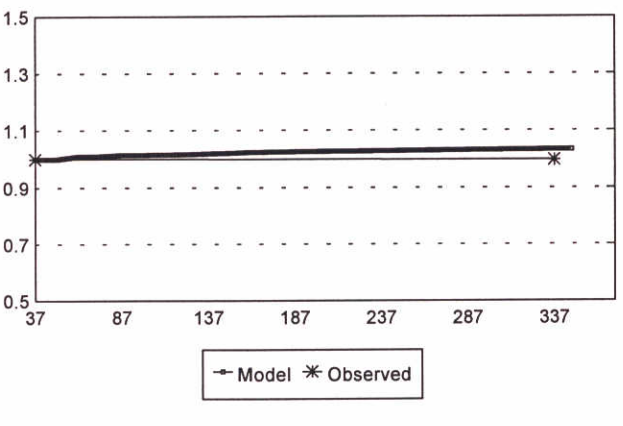

500

Volumetric results 1968 - 1993 Run 500 Areas 4, 5 and 6		Nov 1994
	ESTMORF	
DELFT HYDRAULICS	Z-715	Fig.4.4.11

The Friesche Zeegat before the closure 1957 geometry		Nov 1994
	ESTMORF	
DELFT HYDRAULICS	Z-715	Fig.5.1.1

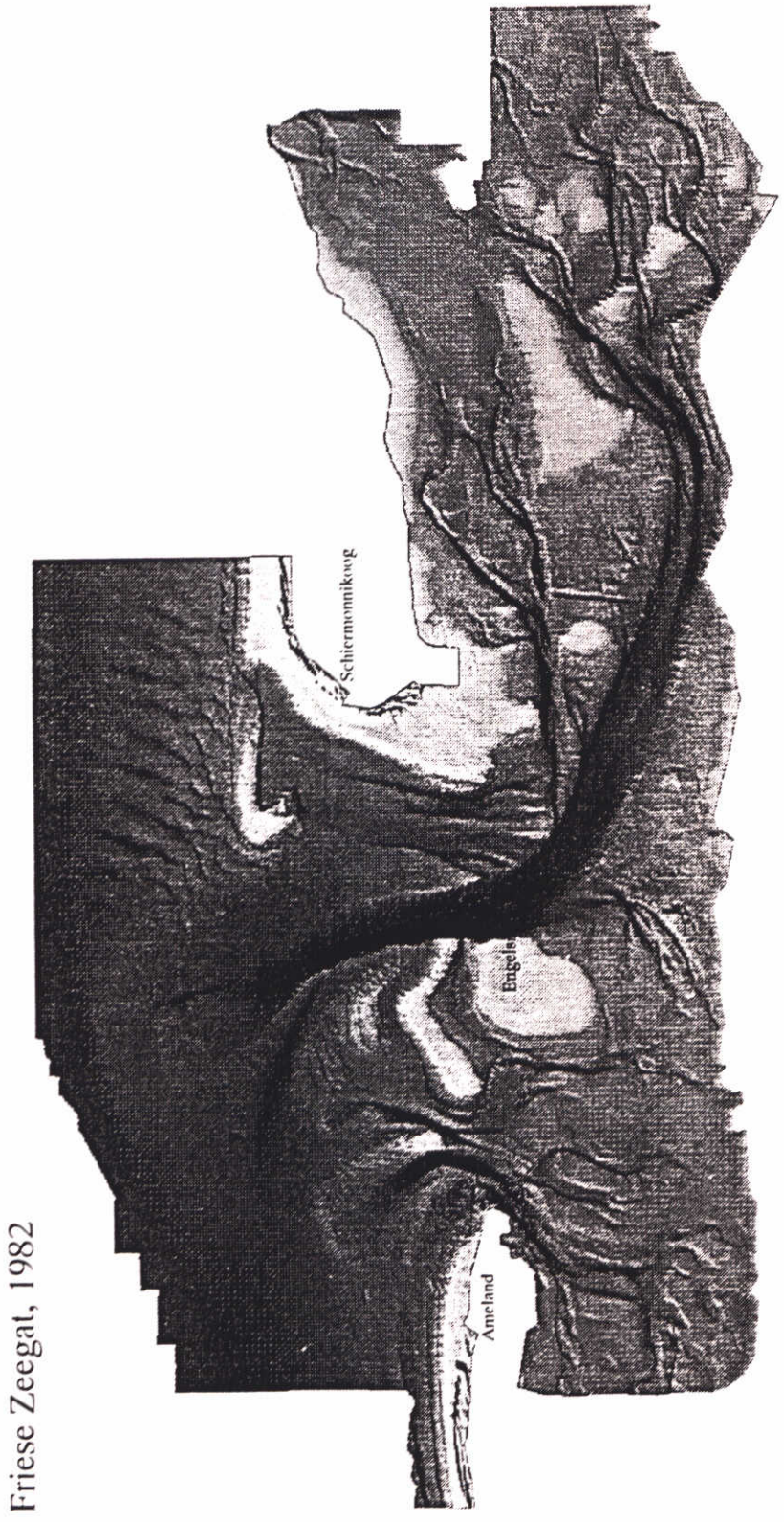

The Friesche Zeegat after the closure 1982 geometry		Nov 1994
	ESTMORF	
DELFT HYDRAULICS	Z-715	Fig.5.1.2

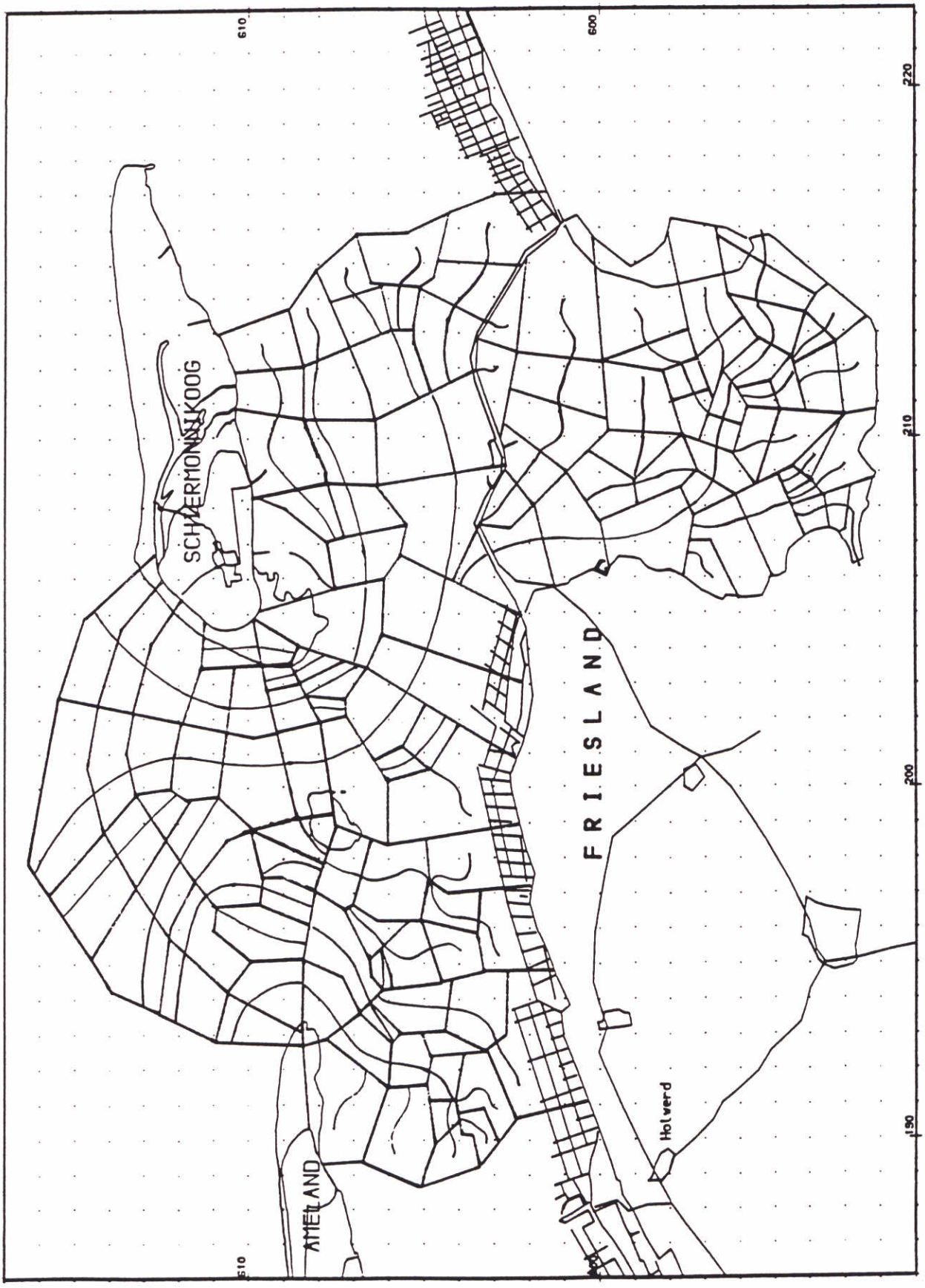

Location of the channels of the Friesche zeegat model.

A4

DELFT HYDRAULICS

Fig 5.2.1

Branch numbers of the Friesche zeegat model.

A4

DELFT HYDRAULICS

Fig 5.2.2

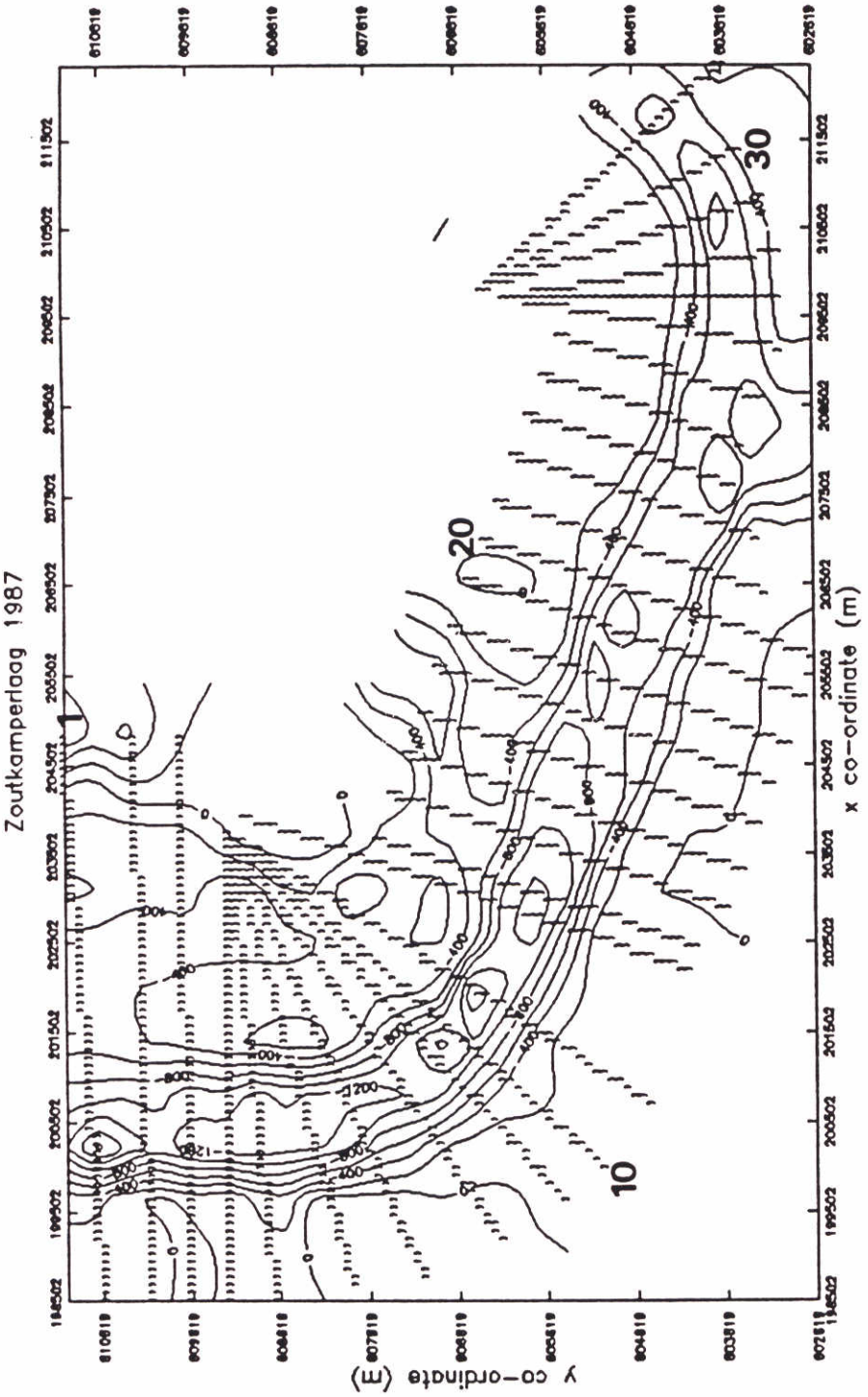

Location of all cross-sectional data for areas.

A4

DELFT HYDRAULICS

Fig 5.3.1

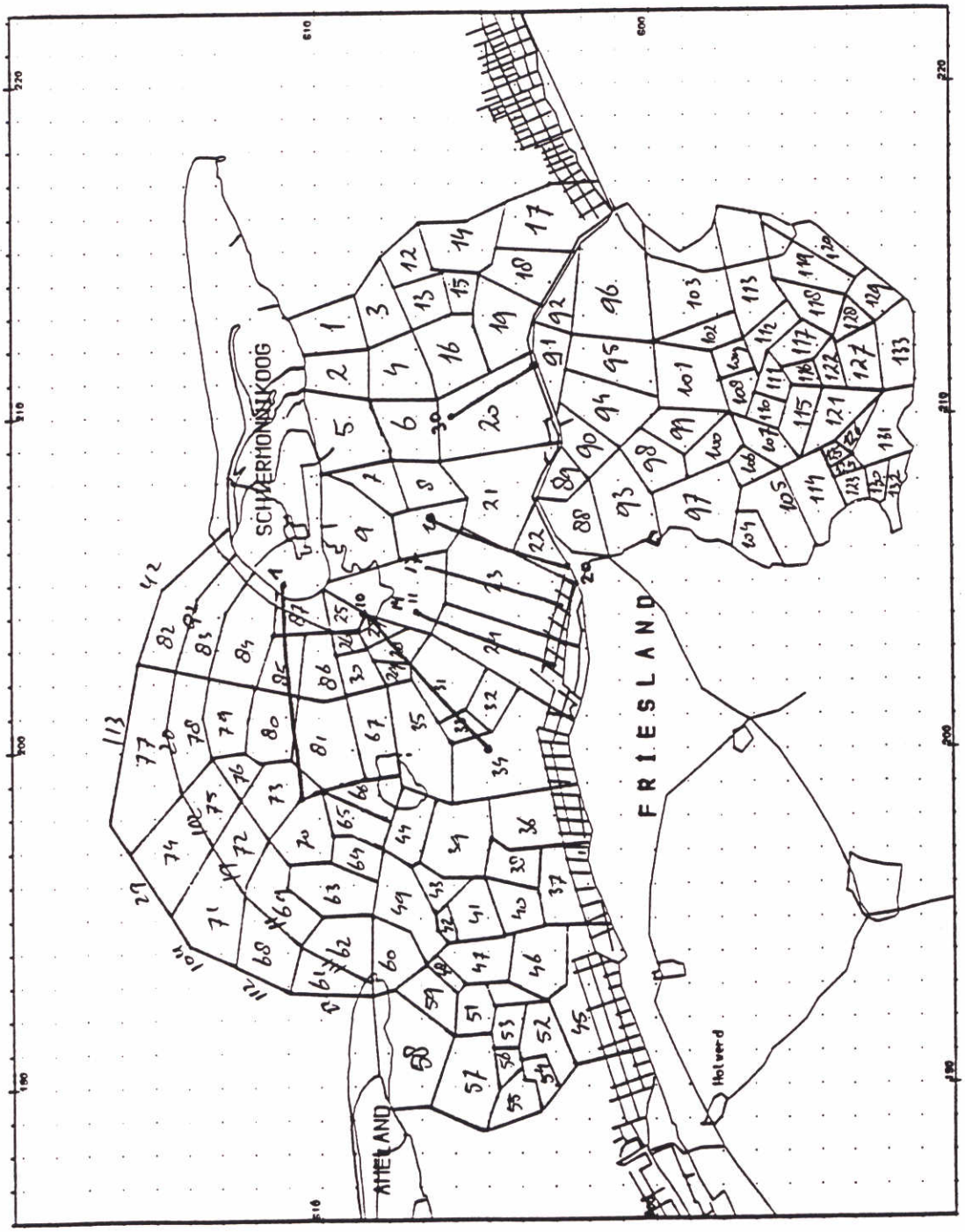

Locations of the selected cross-sections in the model schematization		Nov 1994
	ESTMORF	
DELFT HYDRAULICS	Z-715	Fig.5.3.2

Cross-29/Branch 20

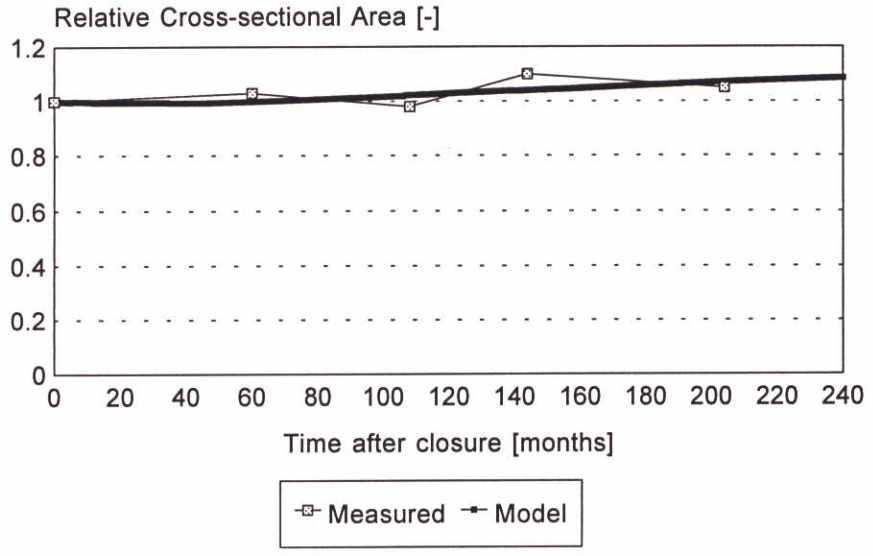

Cross-24/Branch-21

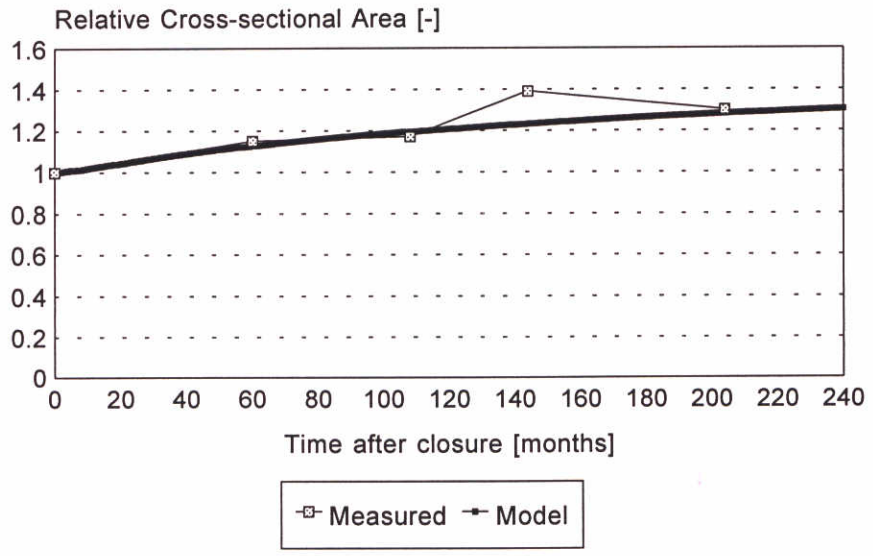

Observed and computed, D_c = 100 m²/s Relative cross-sectional area 1969 - 1988 Branch 20 and 21 of the model	Run 9	Nov 1994
	ESTMORF	
D E L F T H Y D R A U L I C S	Z-715	Fig.5.4.1

Cross-17/Branch-23

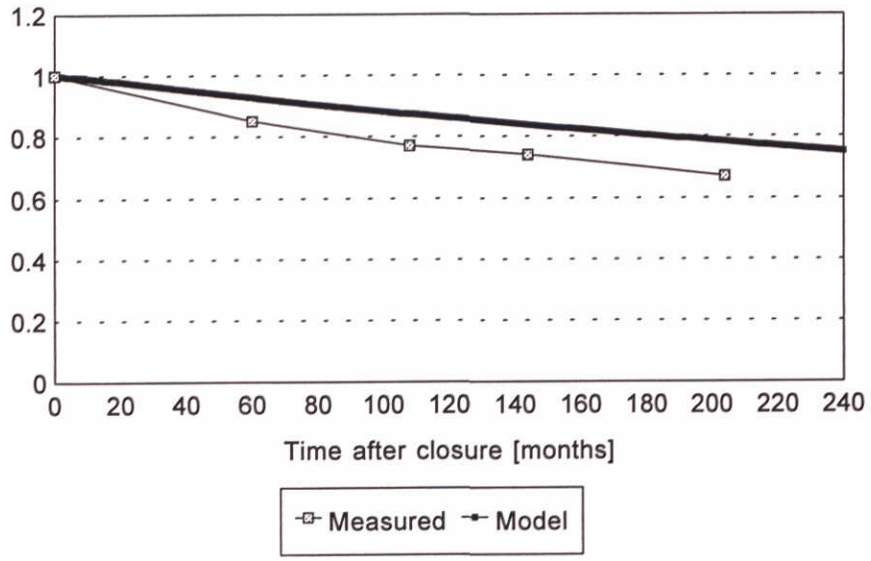

Cross-14/Branch-24

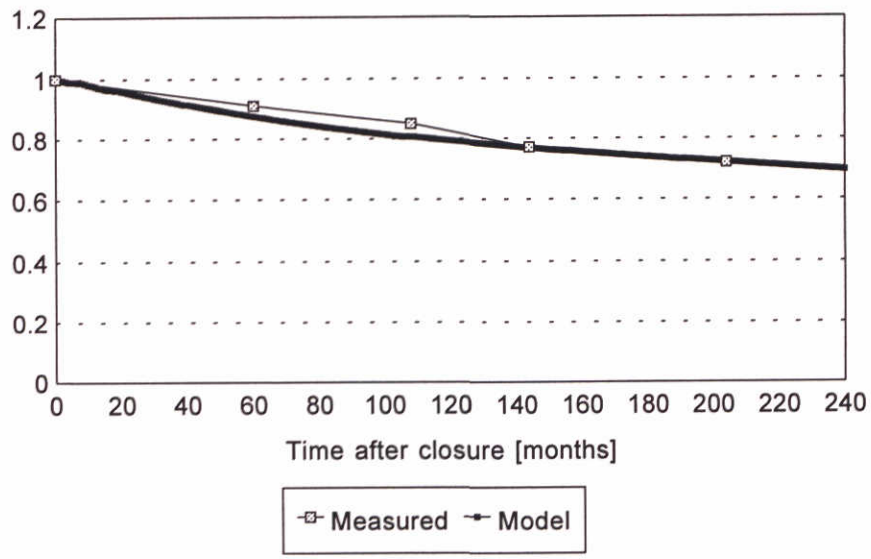

Observed and computed, D_c = 100 m²/s Relative cross-sectional area 1969 - 1988 Branch 23 and 24 of the model	Run 9	Nov 1994
	ESTMORF	
D E L F T H Y D R A U L I C S	Z-715	Fig.5.4.2

Cross-10/Branch-31

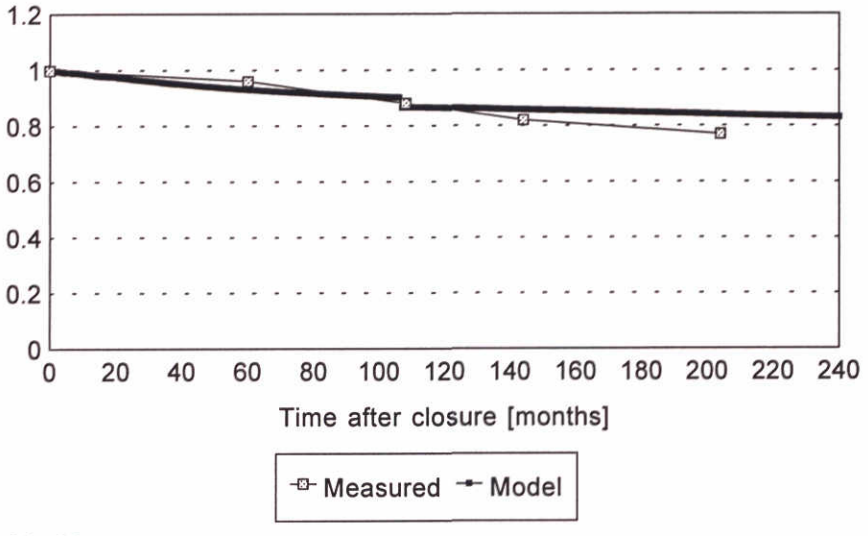

27, 28, 31, 32

Cross-9/Branch-35

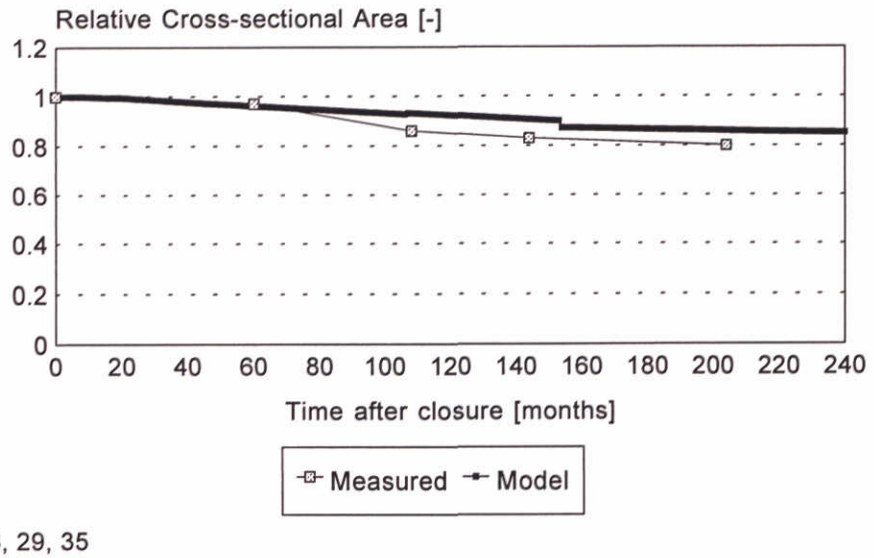

27, 28, 29, 35

Observed and computed, D_c = 100 m²/s Relative cross-sectional area 1969 - 1988 Branch 31 and 35 of the model	Run 9	Nov 1994
	ESTMORF	
D E L F T H Y D R A U L I C S	Z-715	Fig.5.4.3

Cross-6/Branch-67

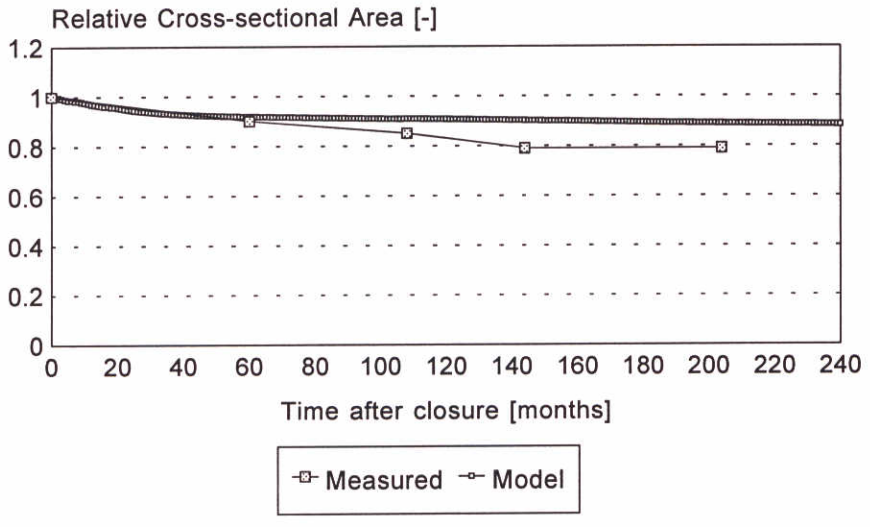

25, 26, 30, 67

Cross-2/Branch-81

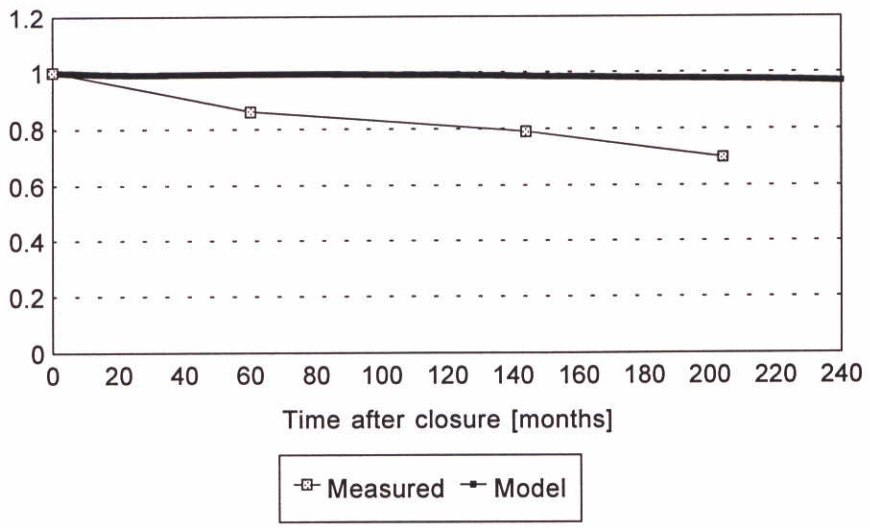

81, 86, 87 combined

Observed and computed, D_c = 100 m²/s Relative cross-sectional area 1969 - 1988 Branch 67 and 81 of the model	Run 9	Nov 1994
	ESTMORF	
D E L F T H Y D R A U L I C S	Z-715	Fig.5.4.4

Cross-29/Branch 20

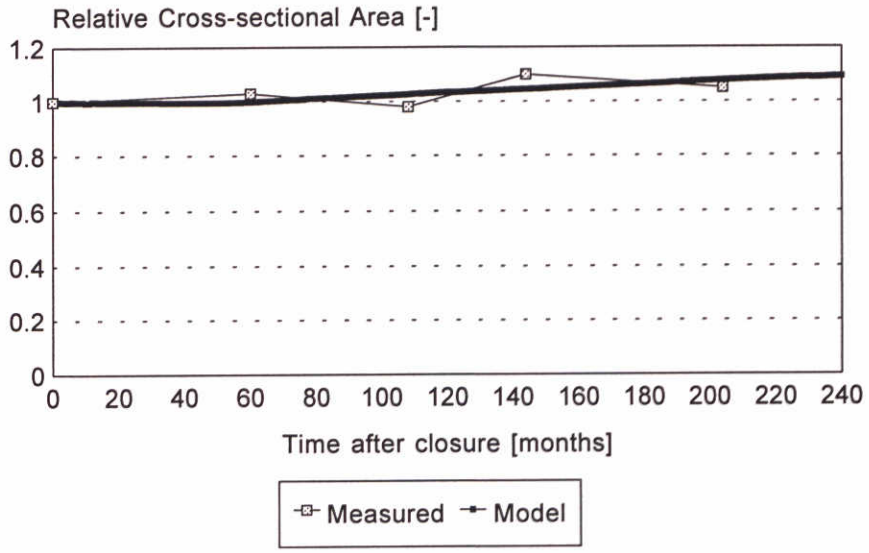

Cross-24/Branch-21

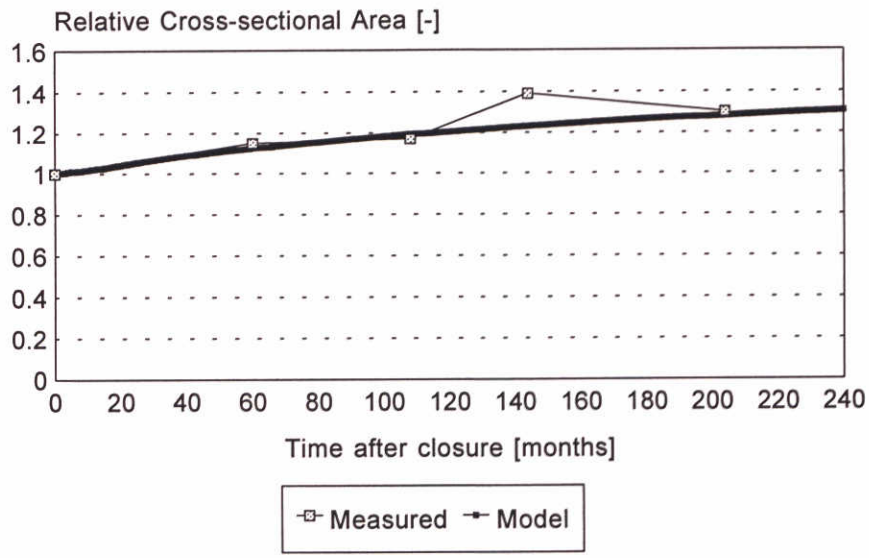

Observed and computed, space-varying D_c Relative cross-sectional area 1969 - 1988 Branch 20 and 21 of the model	Run 11	Nov 1994
	ESTMORF	
D E L F T H Y D R A U L I C S	Z-715	Fig.5.4.5

Cross-17/Branch-23

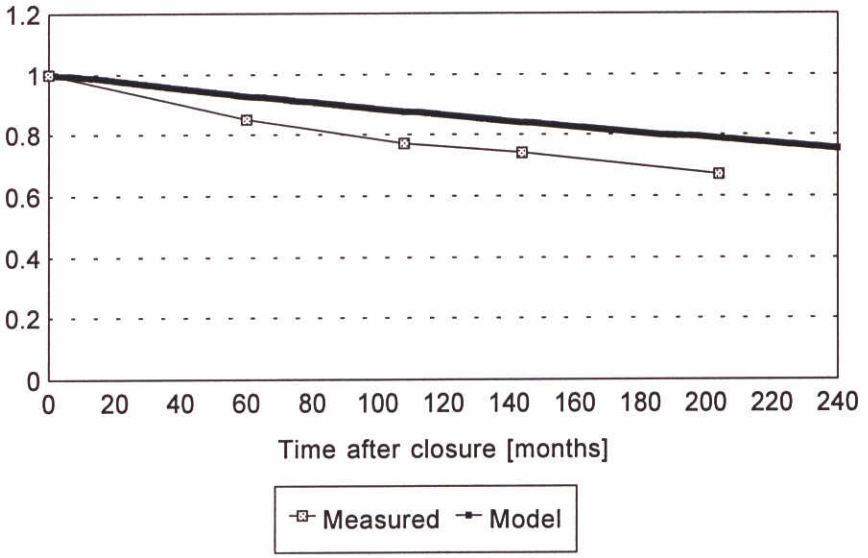

Cross-14/Branch-24

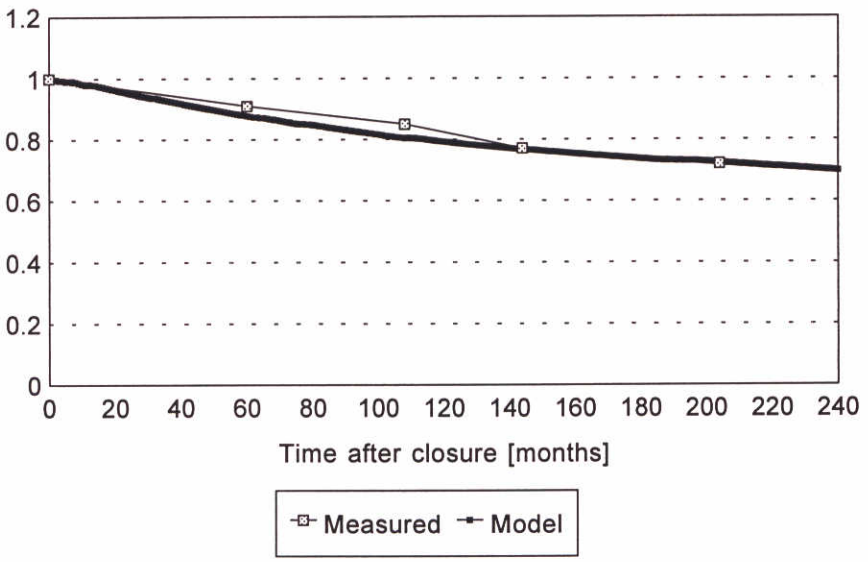

Observed and computed, space-varying D_c Relative cross-sectional area 1969 - 1988 Branch 23 and 24 of the model	Run 11	Nov 1994
	ESTMORF	
DELFT HYDRAULICS	Z-715	Fig.5.4.6

Cross-10/Branch-31

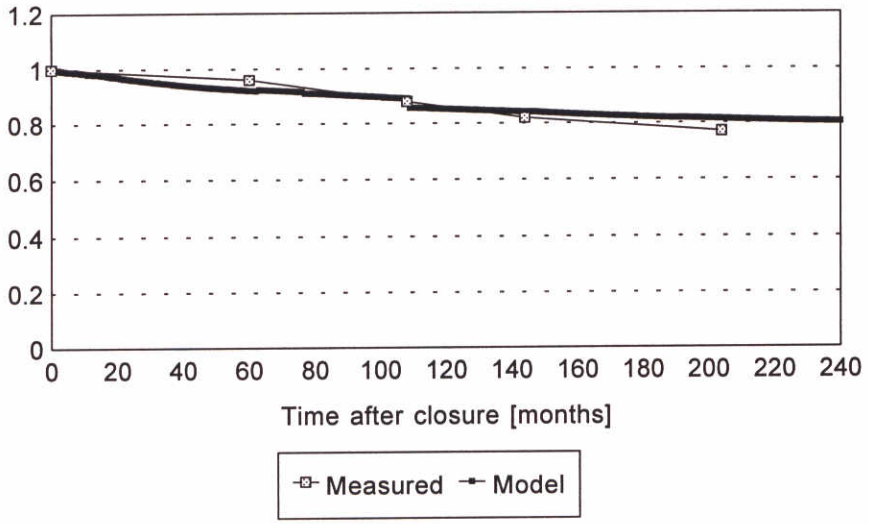

27, 28, 31, 32

Cross-9/Branch-35

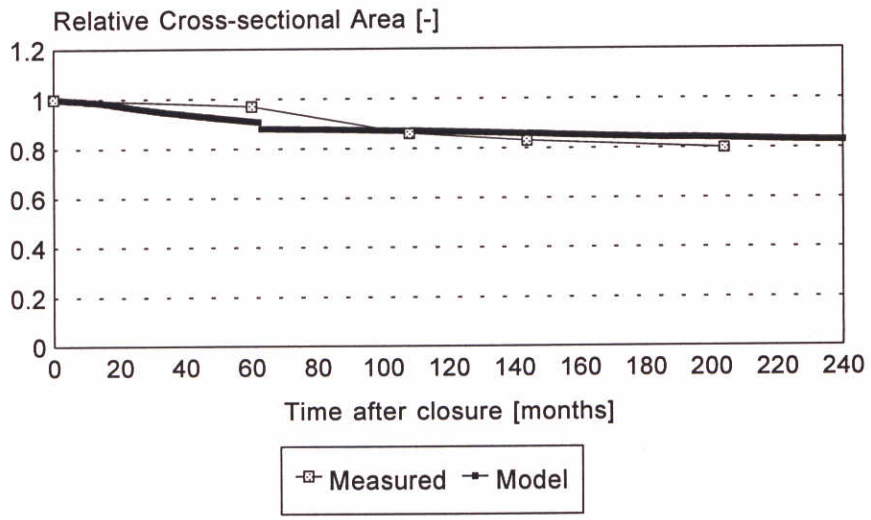

27, 28, 29, 35

Observed and computed, space-varying D_c Relative cross-sectional area 1969 - 1988 Branch 31 and 35 of the model	Run 11	Nov 1994
	ESTMORF	
DELFT HYDRAULICS	Z-715	Fig.5.4.7

Cross-6/Branch-67

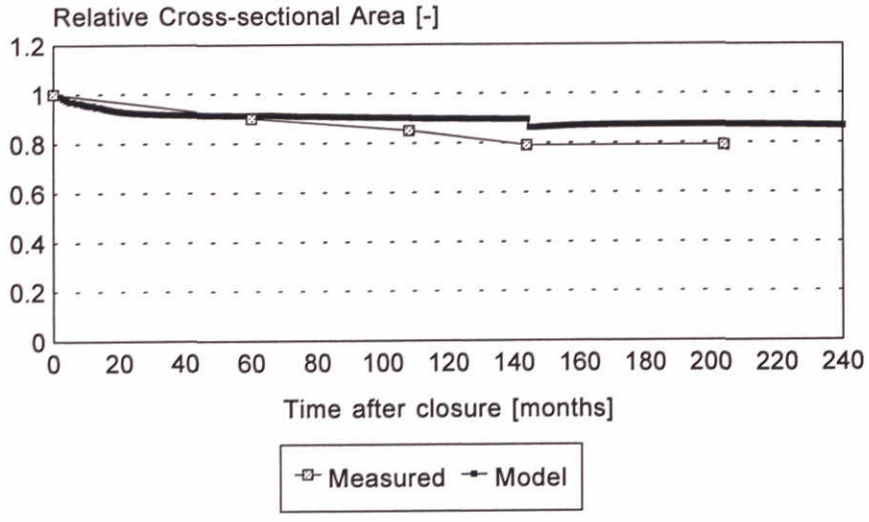

25, 26, 30, 67

Cross-2/Branch-81

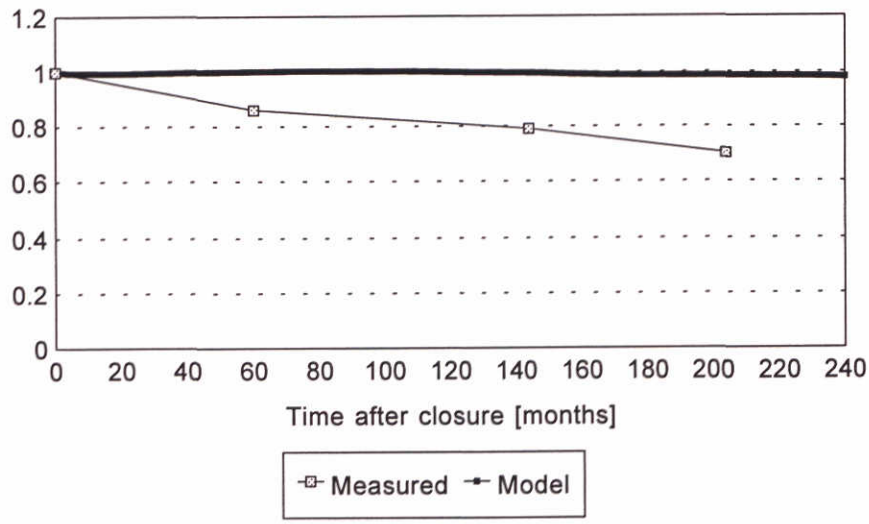

81, 86, 87 combined

Observed and computed, space-varying D_c Relative cross-sectional area 1969 - 1988 Branch 67 and 81 of the model	Run 11	Nov 1994
	ESTMORF	
D E L F T H Y D R A U L I C S	Z-715	Fig.5.4.8

1969

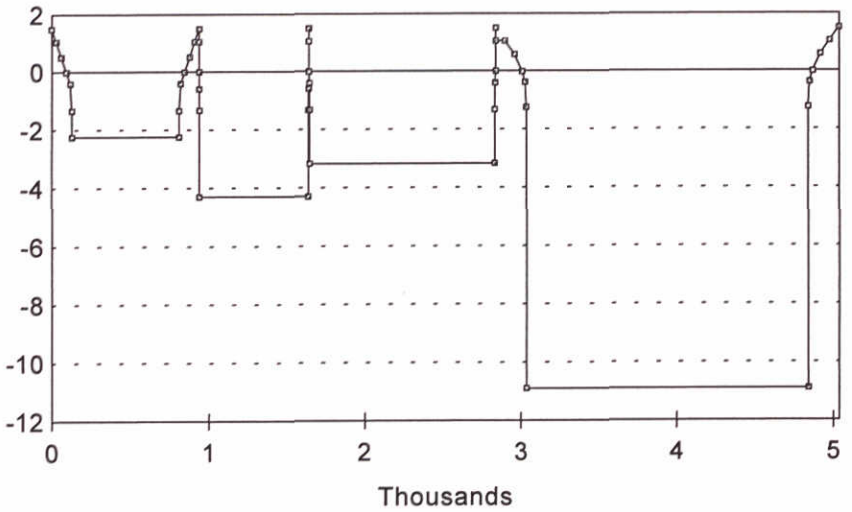

25, 26, 30, 67

1988

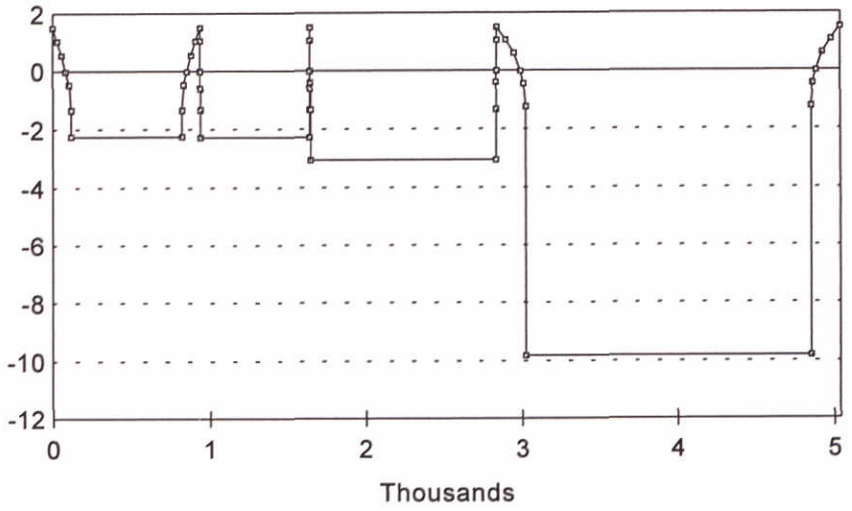

25, 26, 30, 67

Computed cross-sectional profile 1969 and 1988 Entrance of the Friesche Zeegat Run 9		Nov 1994
	ESTMORF	
D E L F T H Y D R A U L I C S	Z-715	Fig.5.4.9

1969

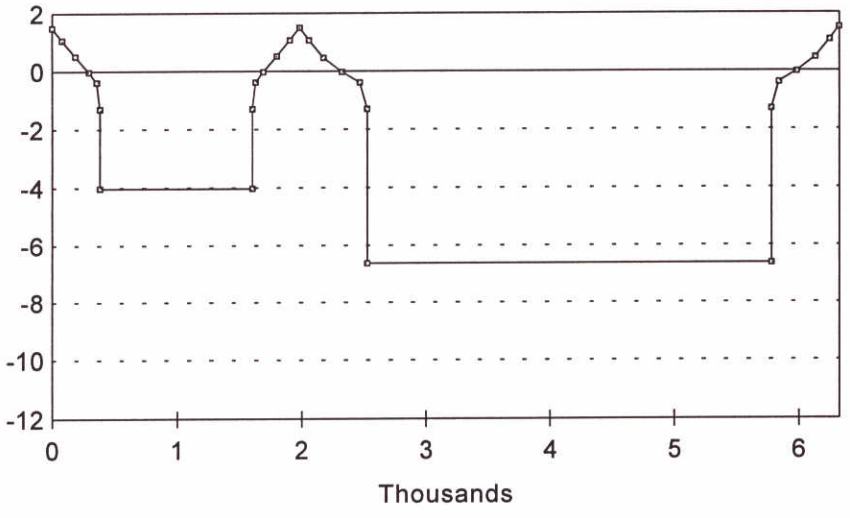

11, 24

1988

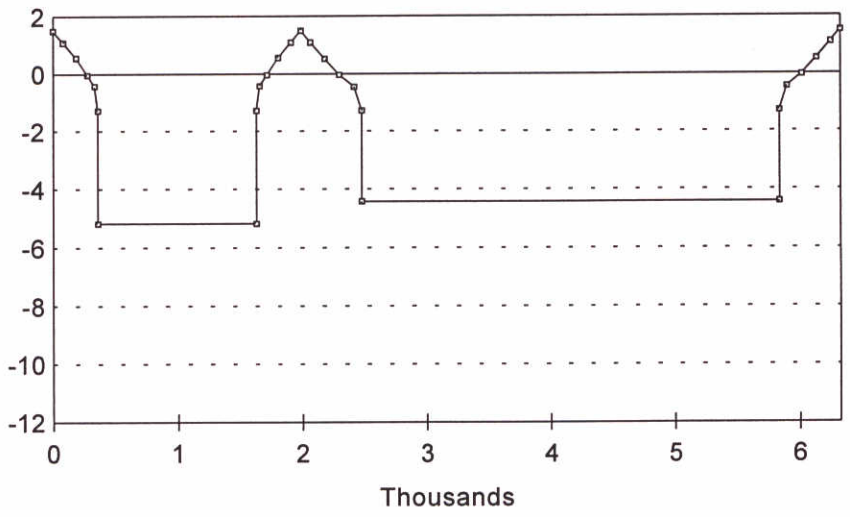

11, 24

Computed cross-sectional profile 1969 and 1988 Middle of Zoutkamperlaag Run 9		Nov 1994
	ESTMORF	
D E L F T H Y D R A U L I C S	Z-715	Fig.5.4.10

1969

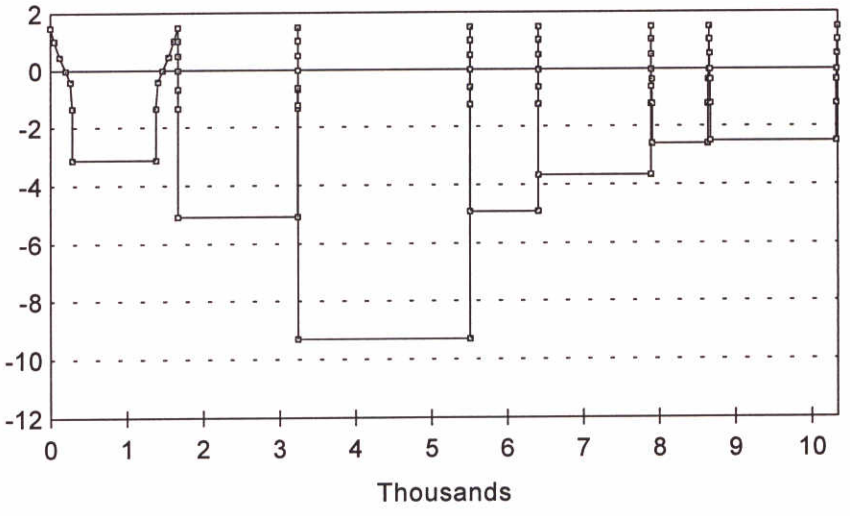

87, 85, 80, 73, 70, 63, 62

1988

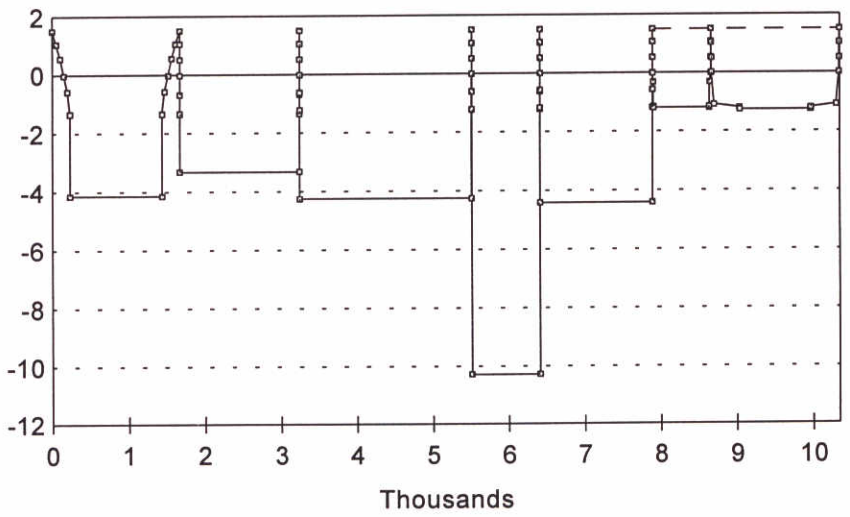

87, 85, 80, 73, 70, 63, 62

Computed cross-sectional profile 1969 and 1988 Ebb tidal delta Run 11		Nov 1994
	ESTMORF	
DELFT HYDRAULICS	Z-715	Fig.5.4.12

main office
Rotterdamseweg 185
p.o. box 177
2600 MH Delft
The Netherlands
telephone (31) 15 - 56 93 53
telefax (31) 15 - 61 96 74
telex 38176 hydel-nl

location 'De Voorst'
Voorsterweg 28, Marknesse
p.o. box 152
8300 AD Emmeloord
The Netherlands
telephone (31) 5274 - 29 22
telefax (31) 5274 - 35 73
telex 42290 hylvo-nl